04268-6-T

THE UNIVERSITY OF MICHIGAN

COLLEGE OF ENGINEERING

DEPARTMENT OF MECHANICAL ENGINEERING
HEAT TRANSFER AND THERMODYNAMICS LABORATORY

Technical Report No. 1

Transient, Laminar, Free-Convection Heat and Mass Transfer in Closed, Partially Filled, Liquid Containers

JOHN A. CLARK
HUSSEIN Z. BARAKAT

Under contract with:

National Aeronautics and Space Administration
George C. Marshall Space Flight Center
Contract No. NAS-8-825
Huntsville, Alabama

Administered through *January 1964*

OFFICE OF RESEARCH ADMINISTRATION · ANN ARBOR

THE UNIVERSITY OF MICHIGAN
COLLEGE OF ENGINEERING
Department of Mechanical Engineering
Heat Transfer and Thermodynamics Laboratory

Technical Report No. 1

TRANSIENT, LAMINAR, FREE-CONVECTION HEAT AND MASS TRANSFER IN CLOSED, PARTIALLY FILLED, LIQUID CONTAINERS

John A. Clark
Hussein Z. Barakat

ORA Project 04268

under contract with:

NATIONAL AERONAUTICS AND SPACE ADMINISTRATION
GEORGE C. MARSHALL SPACE FLIGHT CENTER
CONTRACT NO. NAS-8-825
HUNTSVILLE, ALABAMA

administered through:

OFFICE OF RESEARCH ADMINISTRATION ANN ARBOR

January 1964

TABLE OF CONTENTS

	Page
NOMENCLATURE	v
ABSTRACT	vii
I. INTRODUCTION	
II. REVIEW OF THE LITERATURE	1
A. Analytical Studies	3
B. Experimental Studies	8
III. THEORETICAL ANALYSIS	13
A. Formulation	13
1. Statement and physics of the problem	13
2. General model	14
3. Simplified model	18
B. The Solution	22
C. Finite-Difference Approximations	23
D. Stability and Convergence	27
IV. RESULTS	34
A. The Effect of Gride Size	37
B. Comparison with Experiment	38
V. CONCLUSIONS	40
ACKNOWLEDGMENT	41
REFERENCES	42
APPENDIX. COMPUTER PROGRAM	45

NOMENCLATURE

a	half the width of the container
b	the initial height of the liquid
C_p	constant pressure specific heat, Btu/lbm°F
Gr	Grashof number = $g\beta(T_s-T_o)a^3/\nu^2$
g	the acceleration of gravity, ft/sec^2
h_{fg}	latent heat of evaporation or condensation Btu/lbm
k	thermal conductivity, Btu/hr ft °F
p	pressure
Pr	Prandtl number = γ/α
Ra	Rayleigh number (GrPr)
$(q/A)_w$	heat flux at the walls of the tank per unit area, Btu/hr/ft^2
T	temp R
t	time, sec
u	x-component of the velocity, ft/sec
v	y-component of the velocity, ft/sec
U	dimensionless x-component of the velocity
V	dimensionless y-component of the velocity
x	axial distance, ft
X	dimensionless x
y	transverse, or normal distance measured from center line, ft
Y	dimensionless y

$w = \frac{a^2}{b^2} \frac{\partial^2 \psi}{\partial X^2} + \frac{\partial^2 \psi}{\partial Y^2}$

α thermal diffusivity, ft^2/sec

β coefficient of thermal expansion

ρ density, lbm/ft^3

μ viscosity, lbm/ft/sec

ν kinematic viscosity, ft^2/sec

ϕ dissipation function for two-dimensional incompressible flow is given by

$$\phi = 4\left(\frac{\partial u}{\partial x}\right)^2 + \left(\frac{\partial v}{\partial x} + \frac{\partial u}{\partial y}\right)^2$$

τ dimensionless time

Θ dimensionless temperature

ψ stream function

λ an eigenvalue

Subscripts

c cold wall

g vapor

h hot wall

s saturation or liquid surface

i,j denotes position in the space grid

o denotes initial conditions

w wall

Superscript

n denotes the time level

ABSTRACT

11405

The two-dimensional, laminar, transient, natural convection heat and mass transfer in a closed rectangular container with a free surface is studied. The x-momentum, the y-momentum, and the continuity equations are coupled to obtain the vorticity transport equation, which is integrated numerically using the finite-difference approximation. The problem of stability, which is associated with the difference equations, is studied. The convergence of the solution of the difference equations so that of the differential equation is examined. Results of the calculations for different boundary conditions are given. Comparison of the theoretical results with two experimental measurements from the literature indicate qualitative agreement.

I. INTRODUCTION

This report presents the initial results of a program of research dealing with transient, free convection inside closed containers. The problem reported is the first phase of a program directed at an understanding and prediction of fluid behavior in closed containers subject to various disturbances, including those of ambient heat flux, change in wall temperature, pressurization, change in gravitational field, and liquid discharge. The objectives of the general program are the prediction of transient velocity profiles, temperature stratification, and pressure histories in such containers.

The present report treats laminar transient free convection in a two-dimensional container having a liquid-vapor interface. Transient processes are introduced by a sudden increase in the temperature of the container wall and by a sudden application of heat flux to the external surfaces of the container. For a system at constant pressure and at normal gravity the resulting transient flow patterns and temperature stratification are computed.

The problem is formulated from the complete Navier-Stokes equations coupled with those from the First Law of Thermodynamics and the Conservation of Mass. Boundary-layer approximations are not made since the geometry and boundary conditions invalidate complete boundary-layer flow and require additional momentum considerations not usually found in boundary-layer calculations. Reduction of the governing equations is done by numerical procedures using an IBM 7090 digital computer. Special attention is given to the problem of convergence and stability of the numerical solution.

Combined with the experimental program presently under way, these results will aid in the establishment of criteria for the onset of transition flow in the container, the start of surface boiling, and will be useful in formulating the solution for the case of turbulent convection.

II. REVIEW OF THE LITERATURE

In the past, considerable effort has been given to the study of natural convection heat and mass transfer. Many problems have been solved under different conditions of geometry and arrangements. These studies have been of an analytical as well as an experimental nature. An extensive survey of literature showed that the problem of natural convection in closed-end tubes with a free surface has not been considered analytically, however, some problems with related geometries have been considered. The extrapolation of the results of these studies to other geometry can give misleading results owing to the complicated nature of transient free-convection phenomena.

A. ANALYTICAL STUDIES

The case of a vertical element immersed in an infinite fluid initially at rest has received the most attention of many investigators. The time-steady laminar flow equations were first solved by Pohlhausen[25] for air. The experimental results of Schmidt and Beckman[2] are in good agreement with Pohlhausen's solution. Later, Ostrach[20] solved the same problem using numerical methods with high-speed digital computer for different values of Prandtl number ranging from 0.01 to 1000.

The transient free convection from vertical flat plates, with and without appreciable thermal capacity and variable fluid properties, has been studied by different investigators for different boundary conditions.[8,29,30,33,34]

Leitzke[16] considered the steady-state natural convection between two parallel, infinite flat plates oriented in the direction of body force in which one plate is heated and the other is cooled uniformly. The measured temperature distribution across the fluid is in good agreement with the theory. A generalization of the same problem was carried on by Ostrach,[20,21] in which the plates are maintained at constant temperatures not necessarily equal, and the effect of heat sources and frictional heating was included. As anticipated, the effect of heat sources and viscous heating increases the temperatures and the velocities between the plates. The transient free convection in a duct formed by two infinite parallel plates with arbitrary time variations in the wall temperature and the heat generation was studied by Zeiberg and Mueller.[37]

The two-dimensional steady-state convection in a long rectangle, of which the two long sides are vertical boundaries held at different temperature and the two horizontal boundaries either insulated or have linear temperature distribution, was considered by Batchelor.[1] He did not solve for the velocity or temperature distribution, but he considered the determination of the rate of heat transfer between the two vertical boundaries and the type of different flow regimes that occur for a given value of Rayleigh's number and aspect ratio. For Rayleigh's numbers less than 10^3, Batchelor uses a power series expansion in terms of Rayleigh's number Ra for the dimensionless temperature Θ and the stream function. On substitution of the power series in the governing differential equations and equating coefficients of the like powers of Ra, the problem is reduced to the solution of a series of linear partial differential equations. The Nusselt number, defined as

$$NU = (q/A)_w/K(T_h-T_c) ,$$

is estimated to be of the order

$$NU = \ell/d + 10^{-8} Ra^2 ,$$

where d is the distance between the plates and ℓ the height of the duct. For the case of $\ell/d \to \infty$, he argues that for the regions not near the ends the temperature and the stream function take their asymptotic values, which are given by the solution of two infinite parallel plates, one heated and the other cooled. For infinite values of Ra, he postulates that there is an isothermal core having constant vorticity. He found that the governing equations for the general case could not be represented by a polynomial of small degree nor could they be handled by the Oseen type of linearization.

Foots[26] solved the same problem handled by Batchelor. He obtained a numerical solution based on the use of orthogonal polynomials for the solution of the governing differential equations. Following Batchelor, the stream function and the nondimensional temperature were assumed to be represented by the complete double series of orthogonal functions

$$G = \sum_{n=1}^{\infty} \sum_{m=1}^{\infty} A_{nm} \sin n\pi x \sin m\pi y$$

and

$$\psi = \sum_{n=1}^{\infty} \sum_{m=1}^{\infty} B_{nm} X_n(x) Y_m(y) ,$$

where the A and B are constants which were evaluated numerically. The governing differential equations were reduced to two coupled algebraic equations to be solved simultaneously. The functions $X_n(x)$ were chosen to satisfy the fourth order Sturm-Liouville system and the orthogonality property. The method of solution is tedious, and the calculations are practically impossible for Rayleigh's numbers greater than 10^4 and aspect ratios greater than 4. The results for Rayleigh's number 10^4 and aspect ratio unity are shown in Fig. 14. There is an isothermal core having uniform temperature; there is also a constant vorticity in the core. In the region between the core and the cavity walls, the temperature and the stream function oscillate once near the core and then tend smoothly to their appropriate values at the cavity wall. The boundary layer is continuous between the wall and the core.

Lighthill[18] examined natural convection flows generated by large centrifugal forces in a tube closed at one end and open at the other end to an infinite reservoir, where the tube walls are maintained at a constant temperature. Such a situation exists in cooling gas-turbine blades. He predicted that one of the following three regimes may exist, depending upon the product of Grashof number and the radius-to-length ratio of the tube. The assumed flow regimes are:

1. Similarity flow. For small values of this product, i e., for large values of length-to-radius ratio for a given Grashof number, the boundary layer fills the tube. The velocity and temperature profiles are fully developed. He predicted that for this type of flow, the velocity and temperature distribution are similar at each section of the tube, only their scale is

increasing as the orifice is approached. Assuming that the velocity and temperature vary linearly along the tube, he concluded that there is an aspect ratio for which the temperature changes from its value at the orifice to the value at the bottom. Extending the tube beyond the length determined by the above ratio, the additional length is filled with fluid at rest at the wall's temperature.

2. Boundary-layer type of flow. For high values of the product of Grashof number and radius-to-length ratio, i.e., for short tubes, the flow is of boundary-layer type. In the extreme case, when the boundary layer fills a negligible portion of the tube area, the flow approximates the free-convection flow up a flat plate.

3. Non-similarity regime. This is the type of flow predicted to exist for values of length-to-radius ratio which lie between the values corresponding to the first and the third case. The boundary layer fills a large portion of the tube section. He used the Squire technique to solve the first and the third cases.

Hammitt[9] considered the case of a closed vertical cylinder with internal heat generation. He used the Lighthill technique, modified to account for the heat sources. The agreement between the calculated and measured values of Nusselt's number is not good. This is probably due to some of the inevitable assumptions which are made: (1) small inertia forces compared to buoyancy and shear, (2) radial extend of the temperature and velocity boundary layers is the same, (3) the boundary-layer approximations apply. The first assumption is valid for large Prandtl numbers; the second is valid for

Prandtl numbers near unity. The disadvantage of this method of solution is that it is in capable of detailed examination of the end conditions.

Following Lighthill, Ostrach and Thornton[22] considered a geometrically similar case with a linear wall temperature. In Ostrach's paper, as well as in Lighthill's paper, attention was given to the stagnation of natural convection flows at the closed end. The same problem considered by Lighthill was solved by Levy,[17] using integral methods. He assume that the upward flow consists of a layer of thickness ε near the wall, the remainder of the tube being filled with cold fluid flowing downward. He assumes three regimes of flow similar to those postulated by Lighthill. If the tube length is less than or equal to a length ℓ, the stagnation region does not exist and the upflow convective layer increases with x. For axial distance $x > \ell_1$, ε reaches a constant value d, and such a flow occurs for $\ell_1 < x < \ell_2$. For $x > \ell_2$, there is a stagnation region at the closed section of the tube.

Romonov,[28] also using integral techniques, solved the same problem considered by Lighthill and Levy. His calculations agree with those of Lighthill for infinite Prandtl number, but they differ considerably for Prandtl numbers near unity. The measured and the calculated temperatures are in a good agreement for different wall temperatures.

B. EXPERIMENTAL STUDIES

A large number of experimental studies have involved flat plates immersed in an infinite fluid at rest and either heated or cooled. In general, there has been good agreement between theory and experiment. Considerable experimental work has been done in the field of natural convection in tubes and enclosures. This work has concerned specialized applications and particular configurations. Most of the experiments were in connection with cooling gas-turbine blades and nuclear reactor applications. Although most, if not all, of these experiments are not applicable to this study, they will be helpful in indicating the general trend and the type of experimental equipment required.

Probably the most comprehensive experimental studies of natural convection in thermosyphons are those conducted by Martin[19] in an attempt to check the theoretical work of Lighthill. His results agree qualitatively, although the measured heat-transfer coefficients are nearly twice as large as those predicted by Lighthill. The three regimes predicted by Lighthill were identified from measurements of heat transfer rates. The heat transfer rate was greatest for large values of theproduct of Grashof number and the radius-to-length ratio. The rate was highest at the bottom of the tube, which indicates that there is boundary-layer type of flow. At small values of the product, theheat transfer varied linearly from the orifice to zero at the bottom of the tube, from which Martin concluded that there is a similarity regime. A region of instabilities, characterized by nonsinusoidal oscillatory flow, occurred between the above two steady regimes.

Siegel and Norris[31] shed some light on the oscillatory flow mentioned by Martin by exploring the air flow patterns in the space between two heated wide plates, closed at the bottom, open at the top, and insulated at the sides. For spacing of 0.28 of the plate height, the flow pattern was symmetric, with upward flowing boundary layers near each plate surface and downflow in between. When the spacing was reduced to 0.21 of the height, the flow pattern became asymmetric, with half the cross section occupied by upward (near one plate) and the half near the other plate occupied by downward flow. For smaller spacings, the asymmetric pattern presisted with periodic non-sinusoidal reversal in flow direction and temperature fluctuations.

Curren and Zalabak[4] conducted an experimental investigation to determine the effect of length-to-diameter ratio of closed end coolant passages on natural-convection water cooling of gas turbines. They reported no significant difference in the heat transfer for the different length-to-diameter ratios investigated ranging from 5.1 to 25.5:1. For the largest length-to-diameter ratio, 25.5:1, the boundary layer fills 87% of the tube cross section.

The visual studies of Sparrow and Kauffman[36] of free convection of water in a narrow vertical enclosure, cooled at the top through a copper surface and open at the bottom to a heated reservoir, revealed that the flow pattern is not steady. No region of the enclosure is permanently a region of upflow or of downflow. The size of the various upflow and downflow regions varied along the length of the enclosure at a given time. The number and size of upflow and downflow regions also varied with time. However, end effects were observed, and a continuous downflow took place in a 3/4-inch band adjacent to both walls. Generally, the dominating character of the flow was instability.

Hartnett, et al.,[10,11,15] studied the free-convection heat transfer for the geometry postulated by Lighthill, but with a constant heat flux at the tube wall and water and mercury as working fluids. The effect of inclining the tube was also investigated. Temperature oscillations of the same nature as those reported by Martin and Siegel and Norris were observed. Contrary to the results reported by Curren and Zalabak, the heat transfer was considerably influenced by length-to-radius ratio. A decrease in length-to-radius ratio from 22.5 to 15 results in approximately 100 percent increase in the Nusselts numbers.

Skipper, et al.,[32] studies the natural-convection flow pattern in viscous oil in rectangular tanks heated at the center by vertical coil heater. The flow pattern consisted of a narrow chimney of hot oil rising vertically around and above the heater surface, and a horizontal layer of hot oil at the free surface separated by a sharp vertical gradient from the remaining cold oil below. The hot oil layer had a small vertical temperature gradient, with maximum temperature at the top. The hot oil layer at the surface became increasingly thick with continued heati . The hot oil was found to flow downward at the walls of the tank, while there were suggestions of circulating currents at the side of the rising chimney. The flow pattern shown suggests that a vortex was formed at the free surface near the center line where the hot rising chimney is bifurcated and spread horizontally along the surface. Eichhorn[6] observed similar vortices. These vorticies were formed at the free surface of water near the walls of a cylindrical tube 2 inches diameter and 5-inches long, uniformly heated at the walls and open at the top.

Some of the literature pertaining to the problem at hand will be mentioned later in this study where its application is more important.

[redacted]

III. THEORETICAL ANALYSIS

A. FORMULATION

1. Statement and Physics of the Problem

A closed container is partially filled with a cryogenic liquid. Initially the liquid and the vapor which fills the ullage volume are assumed to be in equilibrium at the temperature T_o, the stauration temperature corresponding to the initial pressure P_o. Previous tests indicate that boiling due to heat leaks from the ambient is a surface phenomenon only; vapor bubble formation is confined to very near the surface; the rest of the liquid does not contain vapor bubbles, and a small change in the ullage pressure is sufficient to cause boiling to cease.[13] From this initial condition, the wall of the vessel is assumed to undergo a step change in temperature or is assumed to be subjected to a uniform heat flux. Simultaneously, the pressure in the ullage volume is changed to P_s, which may be equal to or greater than P_o. The measurements reported in Refs. 3 and 7 indicate that the interface temperature rises very rapidly to T_s, the saturation temperature corresponding to the pressure P_s in the ullage space for these conditions. Buoyant forces, caused by density variations in the liquid, set up natural convection currents. The liquid-vapor system tends to adjust to the new non-equilibrium condition by transferring mass and energy across the interface. The controlling factor is the interface temperature, and each region transfers heat independently of the bulk temperature of the other region. An imbalance of the heat transfer at the liquid-vapor interface is counterbalanced by a phase change, i.e., either transient evaporation or condensation occurs at the interface. In this analysis, the problem is formulated in its general form, taking into consideration the interaction between the liquid and the vapor phase. Later the problem is simplified, making it tractable for analysis without seriously impairing its utility.

2. General Model

Consider a rectangular two-dimensional tank of width 2a and height h.

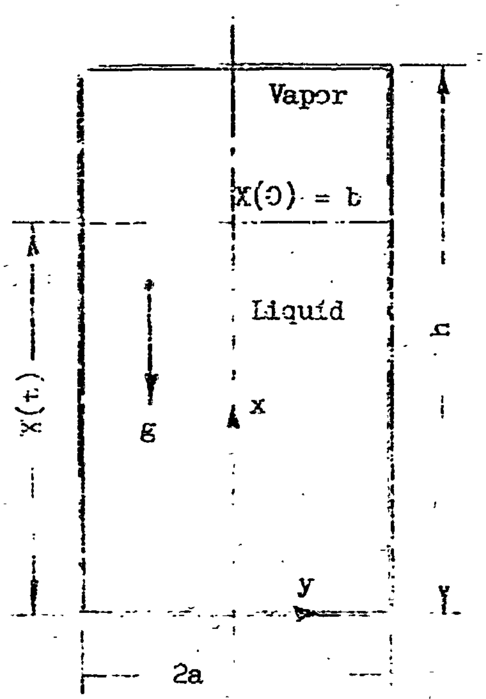

The initial height of the liquid is b, and the depth of the vapor is c. The origin of the coordinate system is taken at the middle of the tank bottom with x positive in the direction of the liquid. The g-level is sufficiently high so that the effect of surface tension can be neglected. The location of the liquid-vapor interface at any one time is given by $x = X(t)$. The two-dimensional transient conditions will be considered.

The differential equations governing the velocity and temperature distribution in the liquid and vapor regions are:

The momentum equations:

The x-momentum equation:

$$\rho\left(\frac{\partial u}{\partial t} + u\,\frac{\partial u}{\partial x} + v\,\frac{\partial u}{\partial y}\right) = -\,\rho g - \frac{\partial p}{\partial x}$$

$$+\,\frac{\partial}{\partial x}\left[\mu\left\{2\,\frac{\partial u}{\partial x} - \frac{2}{3}\left(\frac{\partial u}{\partial x} + \frac{\partial v}{\partial y}\right)\right\}\right] + \frac{\partial}{\partial y}\left[\mu\left(\frac{\partial u}{\partial y} + \frac{\partial v}{\partial x}\right)\right] \qquad (1)$$

The y-momentum equation:

$$\rho\left(\frac{\partial v}{\partial t} + u\,\frac{\partial v}{\partial x} + v\,\frac{\partial v}{\partial y}\right) = -\,\frac{\partial P}{\partial y} + \frac{\partial}{\partial x}\left[\mu\left(\frac{\partial u}{\partial y} + \frac{\partial v}{\partial x}\right)\right]$$

$$+\,\frac{\partial}{\partial y}\left[\mu\left\{2\frac{\partial v}{\partial y} - \frac{2}{3}\left(\frac{\partial u}{\partial x} + \frac{\partial v}{\partial y}\right)\right\}\right] \qquad (2)$$

The energy equation:

$$\rho\, C_p\left(\frac{\partial T}{\partial t} + u\,\frac{\partial T}{\partial x} + v\,\frac{\partial T}{\partial y}\right) = \frac{\partial P}{\partial t} + u\,\frac{\partial P}{\partial x} + v\,\frac{\partial P}{\partial y}$$

$$+\,\frac{\partial}{\partial x}\left(\kappa\,\frac{\partial T}{\partial x}\right) + \frac{\partial}{\partial y}\left(\kappa\,\frac{\partial T}{\partial y}\right) + \mu\,\phi \qquad (3)$$

where, ϕ = dissipation function (see Nomenclature)

The continuity equation:

$$\frac{\partial \rho}{\partial t} + \frac{\partial(\rho u)}{\partial x} + \frac{\partial(\rho v)}{\partial y} = 0 \qquad (4)$$

Initial conditions:

$$T(x,y,o) = T_g(x,y,o) = T_o \tag{5}$$

$$u(x,y,o) = v(x,y,o) = u_g(x,y,o) = v_g(x,y,o) = 0 \tag{6}$$

Boundary conditions:

(a) Velocity boundary conditions.

Assuming the no-slip condition to prevail at the tank walls, the following boundary conditions are obtained:

$$u(o,y,t) = u(x, \pm a,t) = 0 \tag{7}$$

$$v(o,y,t) = v(x, \pm a,t) = 0 \tag{8}$$

$$u_g(h,y,t) = \dot{m}_g/(\rho_g \cdot A) \tag{9}$$

$$u_g(x, \pm a,t) = v_g(x, \pm a,t) = v_g(h,y,t) = 0 \tag{10}$$

Assuming zero shear stress at the liquid-vapor interface, the interfacial boundary conditions could be stated as:

$$u(X,y,t) = u_g(X,y,t) = \frac{dX}{dt} \tag{11}$$

$$\frac{\partial v}{\partial x}(X,y,t) = \frac{\partial v_g}{\partial x}(X,y,t) = 0 \tag{12}$$

From the geometric symmetry of the configuration with respect to the y-axis, it is assumed that the y-component of the velocity vector is zero at the axis of the tank and that the x-component of the velocity is an even function of y, i.e..

$$v(x,o,t) = 0 \tag{13}$$

$$\frac{\partial u}{\partial y}(x,o,t) = 0 \tag{14}$$

(b) Thermal boundary conditions.

The bottom and the upper surface of the tank are either insulated, subjected to a uniform heat flux, or kept at a constant temperature. The walls are either subjected to a uniform heat flux or kept at a constant temperature. Owing to symmetry, the temperature will be an even function of Y.

(1) $$\frac{\partial T}{\partial y}(x,o,t) = \frac{\partial T_g}{\partial y}(x,c,t) = 0 \tag{15}$$

(2) - a. $\frac{\partial T}{\partial x}(o,y,t) = \frac{\partial T_g}{\partial x}(h,y,t) = 0$

b. $k\frac{\partial T}{\partial x}(o,y,t) = k_g\frac{\partial T_g}{\partial x}(h,y,t) = (q/A)_w$

c. $T(o,y,t) = T_g(h,y,t) = T_w$ (16)

(3) - a. $k\frac{\partial T}{\partial y}(x, \pm a,t) = k_g\frac{\partial T_g}{\partial y}(x, \pm a,t) = (q/A)_w$

b. $T(x, \pm a,t) = T_g(x, \pm a,t) = T_w$ (17)

$$(4) \qquad \text{a.} \quad T(X,y,t) = T_g(X,y,t) = T_s$$

$$\text{b.} \quad \frac{\partial T}{\partial x}(b,y,t) = \frac{\partial T_g}{\partial x}(b,y,t) = 0 \tag{18}$$

Any case considered in this work is a combination of the thermal boundary condition, given by Eq. (15), and one of each of the other three boundary conditions given by Eqs. (16), (17), and (18).

Applying the conservation of energy across the interface

$$\rho\, h_{fg}\left(\frac{dX}{dt}\right) = k\left(\frac{\partial T}{\partial x}(X,y,t)\right) - k_g\left(\frac{\partial T_g}{\partial x}(X,y,t)\right) \tag{19}$$

In addition to the boundary conditions stated above, we have the equation of state $P = f(\rho,T)$ for the vapor region. Also, an overall energy and mass balance, considering the system composed of the vapor and liquid regions, is automatically satisfied by any exact solution; it provides a means of checking assumptions or simplifications introduced later in this analysis. As another check on the solution, the net rate of fluid flow across any section of the liquid tank is equal to zero, i.e., $\int_{-a}^{a} u\, dy = 0$

3. Simplified Model

Due to the complexity of the problem, only the liquid region is considered, for which a simplified model is adapted. In reality, the amount of evaporation or condensation is small; therefore, the interfacial displacement is neglected, and the interface is assumed to be always at $x = b$. The pressure of the vapor is considered to be constant; consequently the interface temperature is constant. Constant fluid properties μ, C_p, k and ρ are assumed. Density variations are allowed in the x-momentum equation only. The pressure terms and the dissipation function in the energy equation are neglected.

Initially the pressure throughout the tank is the hydrostatic pressure. The variations in pressure and density caused by the fluid motion and temperature gradients from initial values are expected to be small. Therefore the following assumptions are introduced:

$$P = P_o + P'$$

and

$$\rho = \rho_o + \rho'$$

where P_o is the initial hydrostatic pressure, P' the change in pressure from the initial value, ρ_o initial density, and ρ' the change in density.

Since the pressure variations are small, the density changes due to pressure are negligible, and density variations are caused mainly by temperature changes. Then ρ' can be closely approximated by

$$\rho' = \rho - \rho_o \approx \rho_o \beta(T_o - T) \tag{22}$$

where β is the coefficient of thermal expansion.

Similarly,

$$\frac{\partial P}{\partial x} = -\rho_o g + \frac{\partial P'}{\partial x} \tag{23}$$

$$\frac{\partial P}{\partial y} = \frac{\rho P'}{\partial y} \tag{24}$$

Substituting the above expressions in the momentum equations:

The x-momentum:

$$\rho\left(\frac{\partial u}{\partial t} + u\,\frac{\partial u}{\partial x} + v\,\frac{\partial u}{\partial y}\right) = \rho_o\ \beta g(T-T_o) - \frac{\partial P'}{\partial x} + \mu\left(\frac{\partial^2 u}{\partial x^2} + \frac{\partial^2 u}{\partial y^2}\right) \tag{25}$$

The y-momentum:

$$\rho\left(\frac{\partial v}{\partial t} + u\,\frac{\partial v}{\partial x} + v\,\frac{\partial v}{\partial y}\right) = -\frac{\partial P'}{\partial y} + \mu\left(\frac{\partial^2 v}{\partial x^2} + \frac{\partial^2 v}{\partial y^2}\right) \tag{26}$$

The continuity equation:

$$\frac{\partial u}{\partial x} + \frac{\partial v}{\partial y} = 0 \tag{27}$$

The energy equation:

$$\frac{\partial T}{\partial t} + u\,\frac{\partial T}{\partial x} + v\,\frac{\partial T}{\partial y} = \alpha\left(\frac{\partial^2 T}{\partial x^2} + \frac{\partial^2 T}{\partial y^2}\right) \tag{28}$$

The substitutions necessary to reduce the above differential equations to nondimensionalized forms are:

$$u = \frac{\alpha b}{a^2}\,U \quad , \quad v = \frac{\alpha}{a}\,V$$

$$T-T_o = \frac{\nu\alpha b}{\beta g a^4}\,\Theta \quad , \quad t = \frac{a^2}{\alpha}\,\tau$$

$$x = bX \quad , \quad y = aY \tag{29}$$

S Substituting Eq. (29) in the differential equations, differentiating the x-momentum equation with respect to y and the y-momentum equation with respect to x, combining the two equations, and introducing the stream function, the following equations are obtained:

$$\frac{\partial}{\partial \tau}\left(\frac{a^2}{b^2}\frac{\partial^2\psi}{\partial X^2} + \frac{\partial^2\psi}{\partial Y^2}\right) + \frac{\partial\psi}{\partial Y}\cdot\frac{\partial}{\partial X}\left(\frac{a^2}{b^2}\frac{\partial^2\psi}{\partial X^2} + \frac{\partial^2\psi}{\partial Y^2}\right) - \frac{\partial\psi}{\partial X}\cdot\frac{\partial}{\partial Y}\left(\frac{a^2}{b^2}\frac{\partial^2\psi}{\partial X^2} + \frac{\partial^2\psi}{\partial Y^2}\right)$$

$$= \Pr\frac{\partial\theta}{\partial Y} + \Pr\left[\frac{a^2}{b^2}\frac{\partial^2}{\partial X^2}\left(\frac{a^2}{b^2}\frac{\partial^2\psi}{\partial X^2} + \frac{\partial^2\psi}{\partial Y^2}\right) + \frac{\partial^2}{\partial Y^2}\left(\frac{a^2}{b^2}\frac{\partial^2\psi}{\partial X^2} + \frac{\partial^2\psi}{\partial Y^2}\right)\right] \tag{29a}$$

and

$$\frac{\partial\theta}{\partial\tau} + \frac{\partial\psi}{\partial Y}\frac{\partial\theta}{\partial X} - \frac{\partial\psi}{\partial X}\frac{\partial\theta}{\partial Y} = \frac{a^2}{b^2}\frac{\partial^2\theta}{\partial X^2} + \frac{\partial^2\theta}{\partial Y^2} \tag{30}$$

where the stream function ψ is defined by

$$U = \frac{\partial\psi}{\partial Y}$$

$$V = -\frac{\partial\psi}{\partial X}$$

The initial conditions

$$\theta(X,Y,0) = 0 \tag{31}$$

$$\psi(X,Y,0) = 0 \tag{32}$$

and the boundary conditions are:

$$\psi(X,1,\tau) = \frac{\partial\psi}{\partial X}(X,1,\tau) = \frac{\partial\psi}{\partial Y}(X,1,\tau) = 0 \tag{33}$$

$$\psi(0,Y,\tau) = \frac{\partial\psi}{\partial X}(0,Y,\tau) = \frac{\partial\psi}{\partial Y}(0,Y,\tau) = 0 \tag{34}$$

$$\psi(1,Y,\tau) = \frac{\partial^2\psi}{\partial X^2}(1,Y,\tau) = \frac{\partial^2\psi}{\partial Y^2}(1,Y,\tau) = 0 \tag{35}$$

$$\psi(X,0,\tau) = \frac{\partial^2\psi}{\partial X^2}(X,0,\tau) = \frac{\partial^2\psi}{\partial X^2}(X,0,\tau) = 0 \tag{36}$$

$$\frac{\partial\Theta}{\partial X}(0,Y,\tau) = \frac{\partial\Theta}{\partial Y}(X,0,\tau) = 0 \tag{37}$$

$$\frac{\partial\Theta}{\partial Y}(X,1,\tau) = Gr^* \text{ , or}$$

$$\Theta(X,1,\tau) = \Theta_w \tag{38}$$

$$\Theta(1,Y,\tau) = \Theta_s \text{ , or } \frac{\partial\Theta}{\partial X}(1,Y,\tau) = 0 \tag{39}$$

where:

$$Gr^* = (a/b)Pr\ g\beta a^4(q/A)_w\ (k\nu^2) \tag{40}$$

$$\Theta_s = \frac{a}{b}(T_s - T_o)Pr\ g\beta a^3/\nu^2 = (a/b).Pr.Gr \tag{41}$$

From the above system of equations and boundary conditions, clearly U, V, and Θ are functions of x, y, τ, a/b, Pr, Gr, and Gr*.

B. THE SOLUTION

The nonlinear, fourth order system of Eq. (29a) and (30) is not amenable to mathematical treatment using classical methods. Furthermore, Ostromov[24] and Batchelor[1] found that neither the successive approximation method nor the series expansion is suitable for handling such a system of equations for any arbitrary Pr and Gr. Therefore it was decided to employ a numerical method for the solution; the finite-difference approximation was chosen for the work in this report. The advantage of this method over other numerical methods is that the boundary-layer assumption is no longer necessary. Instead, the full Navier-Stokes equations can be solved. The results obtained by this method can be used to check the validity of the simplifying assumptions made by others.

C. FINITE-DIFFERENCE APPROXIMATIONS

The fourth order, nonlinear system of Eq. (29a) and (30) is transformed to a second order, nonlinear system as follows:

Let

$$w = \frac{a}{b} \frac{\partial^2 \psi}{\partial X^2} + \frac{\partial^2 \psi}{\partial Y^2} \tag{42}$$

Upon substitution in Eq. (29a), the following equation is obtained:

$$\frac{\partial w}{\partial \tau} + U \frac{\partial w}{\partial X} + V \frac{\partial w}{\partial Y} = Pr \frac{\partial \theta}{\partial Y} + Pr\left[\frac{a^2}{b^2} \frac{\partial^2 w}{\partial X^2} + \frac{\partial^2 w}{\partial Y^2}\right] \tag{43}$$

$$\frac{\partial \theta}{\partial \tau} + U \frac{\partial \theta}{\partial X} + V \frac{\partial \theta}{\partial Y} = \frac{a^2}{b^2} \frac{\partial^2 \theta}{\partial X^2} + \frac{\partial^2 \theta}{\partial Y^2} \tag{44}$$

By definition, w is twice the negative of the vorticity, and Eq. (43) is known as the vorticity transport equation. For convenience U and V are substituted for $\partial\psi/\partial Y$ and $-\partial\psi/\partial X$. By this transformation, the system of Eq. (30) and (31) is reduced to three second-order, nonlinear equations which are easier to handle by difference methods compared to the two nonlinear, fourth order Eqs. (29a) and (30).

The differential Eqs. (42) (43), and (44) are approximated by a system of difference equations. Each first order term in Eqs. (43) and (44) can be expressed in forward, backward, or central differences. The choice of the type of difference approximation is determined by whether implicit or explicit difference method is desired and by the stability requirements, to be discussed later. From the beginning of this analysis, explicit methods were felt to be more suitable for handling Eqs. (43) and (44), because the principal interest is in transient phenomena for small physical time. This implies that, for better accuracy, small time steps should be used from the beginning of computation. Desinberre[5] showed that explicit methods are superior to implicit methods as far as accuracy is concerned; he also found that the accuracy requirement restricts the size of the time increment, in the case of implicit methods, to values smaller than required by stability considerations. When explicit methods are used, the nonlinear terms $U(\partial w/\partial X)$, $V(\partial w/\partial Y)$, $U(\partial \theta/\partial X)$, and $V(\partial \theta/\partial Y)$ have to be approximated by forward difference when the sign of the velocity is negative, and by backward difference when the velocity is positive.[35] Central differences are used if implicit schemes are desired. Since the velocity components change sign in the domain ofinterest, four different sets of finite-difference equations are required, and the appropriate set of equations at each location or nodal point is determined accordingly. The four sets of difference equations corresponding to differential Eqs. (43) and (44) are:

(i) $U \geq 0,\ V \geq 0$

$$\frac{w'_{i,j}-w_{i,j}}{\Delta\tau} + U_{i,j}\,\frac{w_{i,j}-w_{i-1,j}}{\Delta X} + V_{i,j}\,\frac{w_{i,j}-w_{i,j-1}}{\Delta Y}$$

$$= Pr\,\frac{\Theta'_{i,j}-\Theta'_{i,j-1}}{\Delta Y} + Pr\left[\frac{a^2}{b^2}\,\frac{w_{i+1,j}-2w_{i,j}+w_{i-1,j}}{(\Delta X)^2} + \frac{w_{i,j+1}-2w_{i,j}+w_{i,j-1}}{(\Delta Y)^2}\right] \tag{45a}$$

$$\frac{\Theta'_{i,j}-\Theta_{i,j}}{\Delta\tau} + U_{i,j}\,\frac{\Theta_{i,j}-\Theta_{i-1,j}}{\Delta X} + V_{i,j}\,\frac{\Theta_{i,j}-\Theta_{i,j-1}}{\Delta Y}$$

$$= \frac{a^2}{\ }\,\frac{\Theta_{i+1,j}-2\Theta_{i,j}+\Theta_{i-1,j}}{(\Delta X)^2} + \frac{\Theta_{i,j+1}-2\Theta_{i,j}+\Theta_{i,j-1}}{(\Delta Y)^2} \tag{46a}$$

(ii) $U \geq 0,\ V \leq 0$

$$\frac{w'_{i,j}-w_{i,j}}{\Delta\tau} + U_{i,j}\,\frac{w_{i,j}-w_{i-1,j}}{\Delta X} + V_{i,j}\,\frac{w_{i,j+1}-w_{i,j}}{\Delta Y}$$

$$= Pr\,\frac{\Theta'_{i,j}-\Theta'_{i,j-1}}{\Delta Y} + Pr\left[\frac{a^2}{b^2}\,\frac{w_{i+1,j}-2w_{i,j}+w_{i-1,j}}{(\Delta X)^2} + \frac{w_{i,j+1}-2w_{i,j}+w_{i,j-1}}{(\Delta Y)^2}\right] \tag{45b}$$

$$\frac{\Theta'_{i,j}-\Theta_{i,j}}{\Delta\tau} + U_{i,j}\,\frac{\Theta_{i,j}-\Theta_{i-1,j}}{\Delta X} + V_{i,j}\,\frac{\Theta_{i,j+1}-\Theta_{i,j}}{\Delta Y}$$

$$= \frac{a^2}{b^2}\,\frac{\Theta_{i+1,j}-2\Theta_{i,j}+\Theta_{i-1,j}}{(\Delta X)^2} + \frac{\Theta_{i,j+1}-2\Theta_{i,j}+\Theta_{i,j-1}}{(\Delta Y)^2} \tag{46b}$$

(iii) $U \leq 0,\ V \geq 0$

$$\frac{w'_{i,j}-w_{i,j}}{\Delta\tau} + U_{i,j}\,\frac{w_{i+1,j}-w_{i,j}}{\Delta X} + V_{i,j}\,\frac{w_{i,j}-w_{i,j-1}}{\Delta Y}$$

$$= \Pr\,\frac{\theta'_{i,j}-\theta'_{i,j-1}}{\Delta Y} + \Pr\left[\frac{a^2}{b^2}\,\frac{w_{i+1,j}-2w_{i,j}+w_{i-1,j}}{(\Delta X)^2} + \frac{w_{i,j+1}-2w_{i,j}+w_{i,j-1}}{(\Delta Y)^2}\right] \tag{45c}$$

$$\frac{\theta'_{i,j}-\theta_{i,j}}{\Delta\tau} + U_{i,j}\,\frac{\theta_{i+1,j}-\theta_{i,j}}{\Delta X} + V_{i,j}\,\frac{\theta_{i,j}-\theta_{i,j-1}}{\Delta Y}$$

$$= \frac{a^2}{b^2}\,\frac{\theta_{i+1,j}-2\theta_{i,j}+\theta_{i-1,j}}{(\Delta X)^2} + \frac{\theta_{i,j+1}-2\theta_{i,j}+\theta_{i,j-1}}{(\Delta Y)^2} \tag{46c}$$

(iv) $U \leq 0,\ V \leq 0$

$$\frac{w'_{i,j}-w_{i,j}}{\Delta\tau} + U_{i,j}\,\frac{w_{i+1,j}-w_{i,j}}{\Delta X} + V_{i,j}\,\frac{w_{i,j+1}-w_{i,j}}{\Delta Y}$$

$$= \Pr\,\frac{\theta'_{i,j}-\theta'_{i,j-1}}{\Delta Y} + \Pr\left(\frac{a^2}{b^2}\,\frac{w_{i+1,j}-2w_{i,j}+w_{i-1,j}}{(\Delta X)^2} + \frac{w_{i,j+1}-2w_{i,j}+w_{i,j-1}}{(\Delta Y)^2}\right) \tag{45d}$$

$$\frac{\theta'_{i,j}-\theta_{i,j}}{\Delta\tau} + U_{i,j}\,\frac{\theta_{i+1,j}-\theta_{i,j}}{\Delta X} + V_{i,j}\,\frac{\theta_{i,j+1}-\theta_{i,j}}{\Delta Y}$$

$$= \frac{a^2}{b^2}\,\frac{\theta_{i+1,j}-2\theta_{i,j}+\theta_{i-1,j}}{(\Delta X)^2} + \frac{\theta_{i,j+1}-2\theta_{i,j}+\theta_{i,j-1}}{(\Delta Y)^2} \tag{46d}$$

The prime refers to the value of the variables at the present time step, and the unprimed variable correspond to those at the previous time step.

The two-dimensional space domain of interest is bounded by $0 \leq X \leq 1$, $-1 \leq Y \leq 1$. Only the region to the right of the x-axis is considered because of geometrical symmetry with respect to this axis. The integers i and j denote the x and y position respectively, with i = 2, j = 2 as the origin, $X = (i-2)$, Δx and $Y = (j-2)$.

D. STABILITY AND CONVERGENCE

The method used in this section follows that of Refs. 27 and 12. The theoretical background for the method may be found in Ref. 27, which presents an excellent discussion of the subject.

Stability is a necessary condition for the solution of the difference equations to converge to the solution of the differential equations as the size of the increments Δx, Δy, and Δt tend to zero. In other words, it is important to identify the behavior of the approximation error as the size of the increments goes to zero and to establish the restrictions to be imposed on the difference equations in order that the error will tend to zero as the increments Δx, Δy, and Δt go to zero. This requires that there be no unlimited amplification of the error as the computing cycles become infinite in the limit.

The Von Neumann method of stability analysis is used in this problem. This method is strictly valid for constant-coefficient difference equations while the equations involved have variable coefficients U and V; however, very good approximation for the stability criterion is obtained by treating the variable coefficients as constants throughout the analysis and then letting the variable coefficients take on their most adverse values in determining the restriction on the time increment size. The fundamentals of the application of this method of stability analysis are best illustrated by the problem in hand. The method will be applied for the case $U \geq 0$, $V \geq 0$. The stability criterion holds irrespective of the sign of U or V. The absolute value of U and V must be used in the equations or inequalities describing the stability criterion, and the appropriate difference equations must be used according to the sign of U and V, as described earlier.

The solution of the difference equations can be written as a Fourier series, the form of which is:[27]

$$w_{i,j}^{(n)} = \sum_{K_1} \sum_{K_2} \xi^{(n)} e^{i(K_1X+K_2Y)} \tag{47}$$

$$\Theta_{i,j}^{(n)} = \sum_{K_1} \sum_{K_2} \mu^{(n)} e^{i(K_1X+K_2Y)} \tag{48}$$

where K_1 and K_2 are integers, n is a superscript denoting the nth time period, and ξ and μ are functions of K_1 and K_2. Substituting the system of Eqs. (47) and (48) into Eqs. (45a) and (46a), the following equations are obtained after some algebraic manipulations:

$$\sum_{K_1}\sum_{K_2}\left\{\xi^{(n+1)} - \xi^{(n)}\left(a_1+a_2\,e^{-iK_1\Delta X} + a_3\,e^{-iK_2\Delta Y} + a_4\,e^{iK_1\Delta X} + a_5\,e^{iK_2\Delta Y}\right)\right.$$

$$\left. + a_6\,\mu^{(n+1)}\right\} e^{i(K_1X+K_2Y)} = 0$$

$$\sum_{K_1}\sum_{K_2}\left\{\mu^{(n+1)} - \mu^{(n)}\left(c_1+c_2\,e^{-iK_1\Delta X} + c_3\,e^{-iK_2\Delta Y} + c_4\,e^{iK_1\Delta X} + c_5\,e^{iK_2\Delta Y}\right)\right\}$$

$$\times\, e^{i(K_1X+K_2Y)} = 0$$

From the above equations, it is concluded that the difference equations are satisfied if

$$\xi^{(n+1)} = \xi^{(n)}\left(a_1+a_2\,e^{-iK_1\Delta X} + a_3\,e^{-iK_2\Delta Y} + a_4\,e^{iK_2\Delta Y} + a_5\,e^{iK_2\Delta Y}\right) + a_6\,\mu \tag{49}$$

and

$$\mu^{(n+1)} = \mu^{(n)}\left(c_1+c_2\,e^{-iK_1\Delta X} + c_3\,e^{-iK_2\Delta Y} + c_4\,e^{iK_1\Delta X} + c_5\,e^{iK_2\Delta Y}\right),$$

where:

$$a_1 = 1 - \left(2\,\frac{a^2}{b^2}\,\frac{Pr}{(\Delta X)^2} + 2\,\frac{Pr}{(\Delta Y)^2} + \frac{|U_{i,j}|}{\Delta X} + \frac{|V_{i,j}|}{\Delta Y}\right)\Delta\tau$$

$$a_2 = \left(\frac{a^2}{b^2}\,\frac{Pr}{(\Delta X)^2} + \frac{|U_{i,j}|}{\Delta X}\right)\Delta\tau$$

$$a_3 = \left(\frac{Pr}{(\Delta Y)^2} + \frac{|V_{i,j}|}{\Delta Y}\right)\Delta\tau$$

$$a_4 = \frac{a^2}{b^2} \frac{Pr}{(\Delta X)^2} \Delta\tau$$

$$a_5 = Pr \frac{\Delta\tau}{(\Delta Y)^2}$$

$$c_1 = 1 - \left(2 \frac{a}{b} \frac{1}{(\Delta X)} + \frac{2}{(\Delta Y)} + \frac{|U_{i,j}|}{\Delta X} + \frac{|V_{i,j}|}{\Delta Y}\right)\Delta\tau$$

$$c_2 = \left(\frac{a^2}{(b\ \Delta X)^2} + \frac{|U_{i,j}|}{\Delta X}\right)\Delta\tau$$

$$c_3 = \left(\frac{1}{(\Delta Y)^2} + \frac{|V_{i,j}|}{\Delta Y}\right)\Delta\tau$$

$$c_4 = \left(\frac{a}{(b\ \Delta X)}\right)^2 \cdot \Delta\tau$$

$$c_5 = \frac{\Delta\tau}{(\Delta Y)^2}$$

No definition has been given to a_6 since it has no effect on this analysis.

The system of Eqs. (49) and (50) are of the form:

$$\xi^{(n+1)} = a_{11}\ \xi^{(n)}(K_1,K_2) + a_{12}\ \mu^{(n)}(K_1,K_2) \tag{51}$$

$$\mu^{(n+1)} = a_{21}\ \xi^{(n)}(K_1,K_2) + a_{22}\ \mu^{(n)}(K_1,K_2) \tag{52}$$

In the matrix notation, the above equalities can be written as

$$\begin{pmatrix} \xi^{(n+1)} \\ \mu^{(n+1)} \end{pmatrix} = \begin{pmatrix} a_{11} & a_{12} \\ a_{21} & a_{22} \end{pmatrix} \begin{pmatrix} \xi^{(n)} \\ \mu^{(n)} \end{pmatrix} \tag{53}$$

The quantity between the first parentheses on the right-hand side of Eq. (53) is called the amplification matrix. The Von Neumann condition necessary for stability is: $|\lambda_{max}| \leq 1$, where λ_{max} is the largest eigenvalue of the amplification matrix. The eigenvalues are given by

$$\begin{vmatrix} a_{11}-\lambda & a_{12} \\ a_{21} & a_{22}-\lambda \end{vmatrix} = 0$$

Substituting the values of a_{11}, a_{12},...etc. in the above determinant and solving for λ, we get

$$\lambda_1 = a_1 + a_2\, e^{-iK_1\Delta Y} + a_3\, e^{-iK_2\Delta Y} + a_4\, e^{iK_1\Delta X} + a_5\, e^{iK_2\Delta Y} \qquad (54)$$

$$\lambda_2 = c_1 + c_2\, e^{-iK_1\Delta X} + c_3\, e^{-iK_2\Delta Y} + c_4\, e^{iK_1\Delta X} + c_5\, e^{iK_2\Delta Y} \qquad (55)$$

The coefficients a_1, a_2,...,c_1,c_2...etc. all are positive except a_1 and c_1, which may be positive or negative. The largest absolute values of λ_1 and λ_2 occur when all the terms in Eqs. (54) and (55) are real, i.e., when $K_1\Delta X$ $K_1\Delta X = K_2\Delta Y = 2\pi$ then,

$$\lambda_{1\,max} = a_1 + a_2 + a_3 + a_4 + a_5 \qquad (56)$$

$$\lambda_{2\,max} = c_1 + c_2 + c_3 + c_4 + c_5 \qquad (57)$$

Substituting the values of a_1, a_2,..., c_1,...,c_5 in λ_{max}

$$\lambda_{1\,max} = \lambda_{2\,max} = 1 \qquad (58)$$

Therefore, we can conclude that λ_{max} will not exceed unity and will not impose any stability restrictions. If there be any restrictions, they are to prevent the minimum value of λ from becoming less than -1.

The minimum of the eigenvalues occurs when $K_1 \Delta X = K_2 \Delta Y = \pi$ and is given by

$$\lambda_{1\,min} = a_1 - a_2 - a_3 - a_4 - a_5$$

$$\lambda_{2\,min} = c_1 - c_2 - c_3 - c_4 - c_5$$

or

$$\lambda_{1\,min} = 1 - 2\,\Delta\tau\left(2\,Pr\left(\frac{a}{b\;\Delta X}\right)^2 + 2\,\frac{Pr}{(\Delta Y)^2} + \frac{|U_{i,j}|}{\Delta X} + \frac{|V_{i,j}|}{\Delta Y}\right) \qquad (59)$$

$$\lambda_{2\,min} = 1 - 2\,\Delta\tau\left(2\left(\frac{a}{b\;\Delta X}\right)^2 + \frac{2}{(\Delta Y)^2} + \frac{|U_{i,j}|}{\Delta X} + \frac{|V_{i,j}|}{\Delta Y}\right) \qquad (60)$$

Therefore, for $|\lambda| \leq 1$, the following inequalities should be satisfied:

$$\Delta\tau\left(\frac{2a^2}{b^2(\Delta X)^2} + \frac{2}{(\Delta Y)^2} + \frac{|U_{i,j}|}{\Delta X} + \frac{|V_{i,j}|}{\Delta Y}\right) \leq 1 \qquad (61a)$$

$$\Delta\tau\left(2\,Pr\left(\frac{a}{b\;\Delta X}\right)^2 + 2\,\frac{Pr}{(\Delta Y)} + \frac{|U_{i,j}|}{\Delta X} + \frac{|V_{i,j}|}{\Delta Y}\right) \leq 1 \qquad (61b)$$

Equations (61a,b) are requisite for stability. For values of Prandtl number less than unity, inequality Eq. (61a) is more restrictive and, therefore, should be used. For higher values of Prandtl number, inequality Eq.(61b) must be used.

The numerical solution is carried as follows:

1. The temperature distribution is first calculated using Eq. (45);

2. The advanced values of temperature Θ' are used in Eq. (46) to calculate w';

3. The stream function is calculated at each time step, using Eq. (42). The solution of Eq. (42) is done numerically, using successive row relaxation followed by successive column relaxation.[36]

IV. RESULTS

Calculations have been carried out for the case of a container with an insulated bottom whose walls are subjected to a uniform heat flux, and the liquid surface is maintained either at the initial temperature T_o, at a temperature, T_s, higher than T_o, or is adiabatic. The last case is expected to approximate the transient convection in the liquid when exposed to a non-pressurized gas. Different levels of heat flux were considered, including 10 and 1000 Btu/hr/ft^2.

For these calculations, the fluid properties chosen were those of liquid nitrogen initially at atmospheric pressure, the initial saturation temperature was 140°R. The fluid properties were evaluated at a temperature equal to the average of the initial temperature and the liquid surface temperature. The values of the liquid properties were taken from Ref. 38 and are summarized in Table I. The height of the liquid b, is 1 ft, and the width of the con-

TABLE I

FLUID PROPERTIES

Thermal diffusivity α, ft^2/sec	8.62×10^{-7}
Thermal conductivity K, Btu/hr/ft^2-°R	0.0775
Kinematic viscosity ν, ft^2/sec	1.68×10^{-6}
Coefficient of thermal expansion, β, °R^{-1}	1.33×10^{-3}
Prandtl number	1.91

tainer is 1/2 ft.

The flow pattern for the case of a constant wall heat flux of 10 Btu/hr/ft^2 and liquid surface maintained at initial temperature T_o is shown in Figs. 1, 2 and 3, using a 21 x 21 grid corresponding to $\Delta X = \Delta Y = 0.05$. These results show the streamline pattern at different time levels—50 sec, 2 min, and 3.6 min respectively. An interesting streamline pattern is observed at the free surface. For a short time after the beginning of heating, the boundary layer rising along the container walls turns smoothly changing its direction from upward to downward flow (Fig. 1). The downward-moving particles near the rising boundary layer reverse direction and join the upward flow, thus giving rise to the vortex near the free surface. The fluid away from the edge of the boundary layer flows nearly to the bottom of the container, where it joins the upward-moving fluid. For greater times following the introduction of the transient, the streamlines near the free surface show the presence of fluid oscillations (Figs. 2 and 3). These oscillations first form near the wall, their amplitude grows with time, and they move towards the centerline of the container. The calculations show that this oscillatory phenomenon is repeated with time in the sequence described (Figs. 2,3,4, and 5).

The effect of increasing the level of heat flux on the flow pattern is clearly shown in Fig. 4, which shows the flow pattern obtained after heating for 51 sec with a wall flux of 1000 Btu/hr/ft^2 and the surface temperature maintained at the initial temperature T_o. The comparison between Figs. 1 and 4, which correspond essentially to the same time, shows that the oscillatory streamline pattern develops earlier for high heating rates than the low heating rates. Except for the latter effect, the flow pattern at the higher heating rates has the same characteristics as that for the low heating rate. The magnitude of the velocities, of course, is higher for the higher heat flux.

The streamlines for the case of a constant wall heat flux of 1000 Btu/hr/ft^2 and adiabatic interface are shown in Fig. 7.

Figures 8 and 9 show the streamlines and the isothermals, respectively, obtained at 1000 Btu/hr/ft^2 wall heat flux and the interface temperature maintained at 160°R, which corresponds to the saturation temperature for a pressure of 45 psia. The axial temperature gradient in the boundary layer is negligible for about 70 percent of the container height at a time of 48 sec. At the upper portion of the container, near the free surface, the axial temperature gradients are considerably greater. On the other hand, the transversal temperature gradient is greater at the lower portion of the tank and becomes smaller near the free surface. The temperature distribution exhibits the same character in all the cases analyzed. These phenomena can be explained as follows: for small times, the fluid near the container walls flows upward in a thin boundary layer. In its upward movement, the hot fluid entrains some of the cold fluid at the edge of the boundary layer. This heated boundary layer is discharged at and just below the free surface, where its transverse velocity is highest. To satisfy continuity, the heated fluid which is discharged at the free surface causes the colder fluid to move downward, thus producing a series of horizontal isotherms. With time these isotherms penetrate further below the free surface. At the lower portion of the container, the transverse temperature gradient is very high near the wall and negligible in the remainder of the container. It is smaller near the free surface, where the boundary-layer flow is discharged. The thermal boundary layer fills the entire cross section in this region.

A. THE EFFECT OF GRID SIZE

Calculations were made for the case of constant wall heat flux of 10 Btu/hr/ft^2 with the fluid surface at its initial temperature, using 21 x 21, 16 x 16 and 11 x 11 grids. The streamline patterns are shown in Figs. 1-4, 6. The oscillatory pattern is obtained in each case, but it is on a smaller scale for the 11 x 11 grid. The axial velocity distribution obtained at a given time is plotted for various axial positions in Fig. 10. The values obtained using 16 x 16 and 21 x 21 are in close agreement. Figure 10 shows that the difference between the values obtained using different grids is greater near the wall and at the center line; otherwise they are in substantial agreement.

Figure 11 shows the dimensionless wall temperature at a location x = .6 plotted against dimensionless time. The deviation is greatest for small times. The difference decreases with time and is practically negligible for dimensionless time of 0.003, which corresponds to about 3.6 min.

Figure 12 presents the velocity at different locations as a function of the grid size. Examination of this figure reveals that the velocities change monotonously with the grid size. Their values are expected to converge to the true solution for a number of divisions of the order of 30 x 30. This is seen from the extrapolation shown as dotted lines in the figures. The rate of convergence is slower near the boundary and at the center than at intermediate positions.

The computations were done on the IBM 7090 digital computer at the Computing Center of The University of Michigan. The machine time required to complete the calculations and to print the results for U,V,T,w, and ψ every 20 steps is 1.7 sec per time step for the 11 x 11 grid. The corresponding times for the 16 x 16 and the 21 x 21 grids are 8 and 11 sec, respectively, for printing the results every five steps.

B. COMPARISON WITH EXPERIMENT

An investigation of the literature on natural convection showed that few present results are applicable to those reported here. These include the work of Eichhorn[6] and S. K. Fenster, et al.,[7] there is other literature concerning flow phenomena in free convection, but, except those cited, none included systems with a free surface.

Eichhorn conducted visual studies of the natural convection laminar flow of water using an electrically heated cylinder 2-inches diameter and 5-inches long. His results are shown in Fig. 13. The magnitude of the heat flux was not given. From the discussion it is concluded that the results represent the unsteady state. Figures 13a and 13b show the flow pattern observed at high heating rate, Fig. 13c shows that obtained at low heating rates. At low heating rates, the streamlines assume a damped-wave shape. At high heating rates, annular vortices repeatedly form near the free surface, roll up until a certain size is reached, whereupon they move away from the cylinder, and another vortex vegins to form. The comparison of Figs. 1-8 with the results of Fig. 13 shows that the shape of streamlines observed agrees with that obtained from the theoretical solutions presented here.

Fenster, et al., studied experimentally the transient phenomena associated with the pressurization of liquid nitrogen initially boiling at constant heat flux. Although the initial temperature distribution agrees with that assumed in this analysis, the initial velocity distribution does not. At any instant after pressurization, there was no difference between the temperature at the tank centerline and midway between the centerline and the wall at an axial location below 0.6 of the liquid height. These results indicate that the isotherms are horizontal in the core of the tank, which agrees with the calculated isotherms shown in Fig. 9.

Temperature oscillations of the type shown in Fig. 9 were also obtained by Poots[26] for the steady state solution of the temperature distribution in a two-dimensional closed cavity. In this case, the walls are kept at a constant temperature, one wall hotter than the other, and the upper and lower surfaces assume a linear temperature distribution. These results are shown in Fig. 14.

V. CONCLUSIONS

The equations describing the transient, two-dimensional, laminar, natural convection in a rectangular closed container having a vapor-liquid interface have been solved using explicit finite-difference approximations. The velocity and temperature distributions indicate that, for small time periods, the flow is of a boundary-layer type, except near the bottom and the liquid-vapor interface. No indications of numerical instability were encountered. The size of the time increment was restricted to small values by stability considerations based on the method of Von Neumann. However, a small time increment is desirable in order to obtain accurate transient results at small time. On the other hand, if steady state results are desired, the number of computations using the explicit method will be large for fine grids and for systems having a high heat flux. The machine time may be of the order of 2 hours in this case,[12] and the use of implicit methods would be superior. However, the application of implicit-difference methods to this problem and to problems with other geometry is being continued.

The results obtained using the present method agree qualitatively with related cases reported in the literature.

ACKNOWLEDGMENT

The authors wish to thank Profs. V. S. Arpaci and W. J. Yang for their valuable suggestions and assistance. The assistance of Professor R.C.F. Bartels, Director of the Computing Center, The University of Michigan, during the initial stages of this work is gratefully acknowledged.

REFERENCES

1. Batchelor, Quart. Applied Math. 12, pp. 209-203, 1954.

2. E. Schmidt and W. Beckmann, Forsch Ing-Wes. 1, 391 (1930).

3. J. A. Clark, G. J. Van Wylen and S. K. Fenster, "Transient Phenomena Associated with the Pressurized Discharge of a Cryogenic Liquid from a Closed Container." Advances in Cryogenic Engineering, 5, pp. 467-480.

4. A. N. Curren and C. F. Zalabak, "Effect of Closed End Coolant Passages on Natural Convection Water Cooling of Gas Turbine Blades." NACA RM R55J 18-a.

5. Dusinberre, "A Note on the "Implicit" Method for Finite-Difference Heat Transfer Calculations." ASME Trans, J. Heat Transfer, Series C, pp. 94-95, Feb. 1961.

6. R. Eichhorn, "Flow Visualization and Velocity Measurement in Natural Convection with Tellurium Die Method." ASME Trans, J. Heat Transfer, 83, Series C, pp. 379-381.

7. S. K. Fenster, G. J. Van Wylen and J. A. Clark, "Transient Phenomena Assoicated with the Pressurization of Liquid Nitrogen Boiling at Constant Heat Flux." Advances in Cryogenic Engineering, 5, pp. 226-234.

8. B. Gebhart, "Natural Convection Transients." ASME Trans., J. Heat Transfer, Series C, 85, pp. 184-185. See also J. Heat Transfer, 85, p. 10 and 83, p. 61.

9. F. G. Hammitt, "Heat and Mass Transfer in Closed, Vertical, Cylindrical Vessels with Internal Heat Sources for Homogeneous Reactors." Ph.D. Thesis, Univ. of Mich., Dec. 1957.

10. J. P. Hartnett, W. E. Welch and F. W. Larsen, "Free Convection Heat Transfer to Water and Mercuty in an Enclosed Cylindrical Tube." Nuclear Engineering and Science Conference, preprint 27, Session XX, Chicago, March 17-21, 1958.

11. J. P. Hartnett and W. E. Welch, "Experimental Studies of Free Convection Heat Transfer in a Vertical Tube with Uniform Heat Flux." Trans, ASME, 79, p. 1651, 1957.

12. J. D. Hellums, "Finite-Difference Computation of Natural Convection Flow." Ph.D. Thesis, Univ. of Mich, Sept. 1960.

13. F. Herzbert, "Effective Density of Boiling Liquid Oxygen." Advances in Cryogenic Engineering, 5.

14. Landau and Lifshitz, "Fluid Mechanics." Adison-Wesly, 1959.

15. F. W. Larsen and J. P. Hartnett, "Effect of Aspect Ratio and Tube Orientation on Free Convection Heat Transfer to Water and Mercuty in Enclosed Circular Tubes." ASME, Trans., J. Heat Transfer, 83, Series C, pp. 87-93.

16. A. F. Leitzke, "Theoretical and Experimental Investigation of Heat Transfer by Natural Convection Between Parallel Plates." NACA Report 1223, 1955.

17. S. Levy, "Integral Methods in Natural Convection Flow." ASME paper No. 55, APM-22.

18. M. J. Lighthill, "Theoretical Consideration on Free Convection in Tubes." Quart. J. Mech. and Appl. Math., 6, pp. 398-439, 1953.

19. B. W. Martin, "Free Convection in an Open Thermosyphen with Special Reference to Turbulent Flow." Proc. Roy. Soc., Series A, 230, pp. 502-530, 1955.

20. S. Ostrach, "An Analysis of Laminar Free Convection Flow and Heat Transfer About a Flat Plate Parallel to the Direction of the Generating Body Force." NACA Report 111, 1953.

21. S. Ostrach, "Laminar Natural Convection Flow and Heat Transfer to Fluids With andWithout Heat Sources With Constant Wall Temperature." NACA Tn-2863, Dec. 1952.

22. S. Ostrach, "Combined Natural and Forced Convection Laminar Flow and Heat Transfer to Fluids With and Without Heat Sources in Channels With Linearly Varying Wall Temperature." NACA Tn-3141, April 1954.

23. S. Ostrach and P. R. Thronton, "On the Stagnation of Natural Convection Flows in Closed End Tubes." ASME paper No. 57-SA-2.

24. G. A. Ostromov, "Free Convection Under the Conditions of the Internal Problem." NACA TM-1407.

25. E. Pohlhausen, ZAMM1, 115 (1921).

26. G. Poots, "Heat Transfer by Laminar Free Convection in Enclosed Plane Gas Layers." Quart. J. Mech. and Appl. Math., XX, Pt. 3, pp. 257-273, 1958.

27. R. D. Richtmyer, "Difference Methods for Initial Value Problem." Interscience Publication, 1957.

28. A. G. Romonov, "Study of Heat Exchange in a Deal End Channel Under Free Convection Conditions." Izvestiya Akademii Nau, USSR. Otdeleni Tekhnishe-kikh, No. 6, pp. 63-76, 1956.

29. R. S. Schechter, "Natural Convection Heat Transfer in Regions of Maximum Fluid Density." AIChE paper No. 57-HT-25.

30. R. Seigel, "Transient Free Convection from a Vertical Flat Plate." ASME paper No. 57-Sa-8.

31. R. Seigel and R. H. Norris, "Test of Free Convection in a Partially Enclosed Spaces Between Two Heated Vertical Plates." ASME paper No. 56-SA-5.

32. R.G.S. Skipper, I.S.C. Holt and O. A. Saunders, "Natural Convection in Viscous Oil." International Development in Heat Transfer, Pt.5, pp. 1003-1009.

33. E. M. Sparrow and J. L. Gregg, "The Variable Fluid Property." ASME paper No. 57-A-46.

34. E. M. Sparrow, J. L. Gree, "Similar Solutions for Free Convection from a Nonisothermal Vertical Plate." ASME paper No. 57-SA-3.

35. E. M. Sparrow and S. J. Kaufmann, "Visual Study of Free Convection in a Narrow Vertical Enclosure." NACA RM E55 L 14-a, Feb. 1956.

36. J. Todd, "Survey of Numerical Analysis." McGraw-Hill, Chap. 11, 1962.

37. S. L. Zeiberg and W. K. Mueller, "Transient Laminar Combined Free and Forced Convection in a Duct." ASME Trans., J. Heat Transfer, 84, Series C, pp. 141-148.

38. "A Compendium of the Properties of Materials at Low Temperature Phase I and II." R. B. Stewart and V. J. Johnson, Editors.

APPENDIX

COMPUTER PROGRAM

The computer program used for the cases of constant wall flux or constant step change in wall temperature and the interfacial temperature specified is given on the following pages. The program is written in MAD language. The symbols U,V,T,W,T_C,T_S,k,A, and B are the same as in the text. The meaning of the principal symbols which are not defined in the program are given below:

Dx	=	Δx
Dy	=	Δy
DT	=	ΔT
M	=	No. of divisions in the x-direction
N	=	No. of divisions in the y-direction
GA	=	Acceleration due to gravity
SF	=	Stream function
ST	=	The value of the stream function at the previous time step
W	=	The value of W at the previous time step
WL	=	The value of W at the advanced time step
TL	=	The value of temperature at the previous time step
NT	=	Total number of time steps
NE	=	Number of interations
TJI	=	Dimensionless wall temperature T_W for the case of step change in wall temperature
TI	=	Dimensionless interfacial temperature.

```
  HUSSEIN Z. BARAKAT               S265F                    020   300
```

```
  HUSSEIN Z. BARAKAT               S265F                    020   300
```


```
$COMPILE MAD,EXECUTE,DUMP,PRINT OBJECT,PUNCH OBJECT
           DIMENSION U(2000,DIM),V(2000,DIM),TL(2000,DIM),T(2000,DIM),
          1ST(2000,DIM),SF(2000,DIM),WL(2000,DIM),W(2000,DIM),DI(100),
          2 EI(100),EJ(100), F(100)
            VECTOR VALUES DIM=2,1,0
           INTEGER I,J,M,N,NT,NE,N1,N2,N3,I1,I3,I4,N4,NTC,J2 ,M5,N5,N6,
          1 N7,N8
           EXECUTE FTRAP.
START       READ AND PRINT DATA
            DIM(2)=N+2
           EXECUTE ZERO.(U(2,2)...U(M+2,N+2),V(2,2)...V(M+2,N+2),T(1,1).
          1..T(M+2,N+2),TL(1,1)...TL(M+2,N+2),ST(2,2)...ST(M+2,N+2),
          2SF(2,2)...SF(M+2,N+2),W(2,2)...W(M+2,N+2),WL(2,2)...WL(M+2,
          3N+2),EI(1)...EI(N+2),DI(1)...DI(N+2),F(1)...F(N+2) ,EJ(1)...
          4  EJ(M+2))
            TC=TC
            TS=TS
            QSURF=QSURF
              A=A
            K=K
           TIME=0
           NT=0
           DX=1./M
           DY=1./N
           I1=M/2
           J2=N/2
             R=AOVERB
           DX2=DX*DX
           DX3=DX2*DX
           DY2=DY*DY
           DY3=DY2*DY
           DXY=DX2/DY2
            DYX=DY2/DX2
            BI=2.*(1+DXY)
            BJ=2.*(1.+DYX)
           C1=GA*PR*BEITA*QSURF*(A.P.4)*R/K/NEW/NEW
             THROUGH ZZ,FOR J=3,1,J.G.N+1
            EI(2)=0
ZZ          EI(J)=1./(BJ-EI(J-1))
             THROUGH VV,FOR I=3,1,I.G.M+1
            EJ(2)=0
VV          EJ(I)=1./(BI-EJ(I-1))
           THROUGH THETAA,FOR I=2,1,I.G.M+2
THETA       TL(I,N+2)=TJ1
           NTC=0
BHACK       NTC=NTC+1
           THROUGH BEHH,FOR J=2,1,J.G.N+3
           TL(M+2,J)=T1
BEHH       T(M+2,J)=T1
           THROUGH ALEFF,FOR I=2,1 ,I.G.M+1
ALEFF       T(I,N+2)=TL(I,N+2)+2.*C1*DT3/DY+TC*DT3*2.*(TL(I,N+1)-
          1TL(I,N+2))/DY2+TC*DT3*R*R*(TL(I+1,N+2)-2.*TL(I, N+2)+TL(I-1,
          2N+2))/DX2
                I(1,N+2)=T(3,N+2)
           THROUGH AALEF,FOR I=2,1,I.G.M+1
            THROUGH AALEF,FOR J=2,1,J.G.N+1
           T(I,J)=TL(I,J)+DT3*R*R*(TL(I+1,J)-2.*TL(I,J)+TL(I-1,J))/DX .
```

```
              1-DT3*(TL(I,J+1)-2.*TL(I,J)+TL(I,J-1))/DY2
              T(I,J)=T(3,J)
               T(1,1)=T(3,1)
   ALEF       T(I,1)=T(I,3)
              THROUGH XX,FOR I=1,1,I.G.M+1
              THROUGH XX,FOR J=1,1,J.G.N+2
   XX          TL(I,J)=T(I,J)
              WHENEVER [illegible] TRANSFER TO BACK
   BACK        [illegible]
              THROUGH SIGMA,FOR [illegible] J.G.N+2)
              THROUGH SIGMA,FOR J=1,1,J.G.N+2
   SIGMA       TL(I,J)=[illegible]
              WHENEVER [illegible].G.N1,DT=DT1
               SMAX=0
              THROUGH GAMMA,FOR I=3,1,I.G.(M+1)
              THROUGH GAMMA,FOR J=3,1,J.G.(N+1)
               WHENEVER PR.L.1
              S=R*R*2./DX2+R*R*2./PR/DY2+.ABS.U(I,J)/DX+.ABS.V(I,J)/DY
              OTHERWISE
              S=R*R*2./DX2+2./DY2+.ABS.U(I,J)/DX+.ABS.V(I,J)/DY
               END OF CONDITIONAL
              WHENEVER SMAX.L.S,
              SMAX=S
   GAMMA       END OF CONDITIONAL
              SN=DT*SMAX
              WHENEVER SN.G.1.,DT=1./SMAX
              TIME=TIME+DT
              THROUGH BEH,FOR J=1,1,J.G.N+2
              T(M+2,J)=T1
   BEH        TL(M+2,J)=T1
              THROUGH ALEF,FOR I=2,1,I.G.(M+1)
   ALEF        T(I,N+2)=TL(I,N+2)+2.*DT*[illegible]/DY+TC*DT*2.*(TL(I,N+1)-
             1TL(I,N+2))/DY2+TC*DT*R*R*(TL(I+1,N+2)-2.*TL(I,N+2)+TL(I-1,
             2N+2))/DX2
              THROUGH DELTA,FOR I=2,1,I.G.(M+1)
              THROUGH DELTA,FOR J=2,1,J.G.N+1
              WHENEVER U(I,J).GE.0
              BT=TL(I,J)-TL(I-1,J)
              OTHERWISE
              BT=TL(I+1,J)-TL(I,J)
              END OF CONDITIONAL
              WHENEVER V(I,J).GE.0
              CT=TL(I,J)-TL(I,J-1)
              OTHERWISE
              CT=TL(I,J-1)-TL(I,J)
              END OF CONDITIONAL
              T(I,J)=TL(I,J)+DT*(T(I+1,J)-2.*T(I,J)+T(I-1,J))*R*R/DX2+DT*(
             1T(I,J+1)-2.*T(I,J)+T(I,J-1))/DY2-U(I,J)*DT*BT/DX-V(I,J)*DT*C
             2T/DY
              T(1,J)=T(3,J)
   DELTA       T(I,1)=T(I,3)
              T(1,N+2)=T(3,N+2)
               T(1,1)=T(3,1)
                WHENEVER NT.G.N5,EPSLN3=EPSLN4
              THROUGH YY,FOR I=3,1,I.G.M+1
              THROUGH YY,FOR J=3,1,J.G.N+1
              W(I,N+2)= -TM*U(I,N+1)/DY
              W(2,J)=-TM*V(3,J)/DX
              WHENEVER U(I,J).GE.0
```

```
            B=(W(I,J)-W(I-1,J))/DX
            OTHERWISE
            B=(W(I+1,J)-W(I,J))/DX
            END OF CONDITIONAL
            WHENEVER V(I,J).GE.0
            C=(W(I,J)-W(I,J-1))/DY
            OTHERWISE
            C=(W(I,J+1)-W(I,J))/DY
            END OF CONDITIONAL
            D=(W(I+1,J)-2.*W(I,J)+W(I-1,J))/DX2
            E=(W(I,J+1)-2.*W(I,J)+W(I,J-1))/DY2
            WL(I,J)=W(I,J)+DT*(R*R*D+E)*PR+PR*DT*(T(I,J)-T(I,J-1))/DY
           1-U(I,J)*DT*B-V(I,J)*DT*C
            WL(I,N+2)=W(I,N+2)
YY          WL(2,J)=W(2,J)
            NE=0
JJ          NE=NE+1
            WHENEVER NE.G.NO
            PRINT RESULTS NE,NE, NT,TIME,SF(2,2)...SF(M+2,N+2),ST(2,2)
           1 ...ST(M+2,N+2),RMAX
            TRANSFER TO EE
            END OF CONDITIONAL
            I=2
II          I=I+1
            I4=I
            THROUGH LM,FOR J=3,1,J.G.N+1
            DI(J)=(ST(I-1,J)+ST(I+1,J))*DYX-DY2*WL(I,J)
            F(2)=0
LM          F(J)=(DI(J)+F(J-1))*EI(J)
            THROUGH LN,FOR J=1,1,J.G.N-1
            I=I4
            H=N+2-J
            SF(I,H)=FI(H)*SF(I,H+1)+F(H)
LN          ST(I,H)=SF(I,H)
            WHENEVER I.L.M+1,TRANSFER TO II
            J=2
HH          J=J+1
            I4=J
              THROUGH MM,FOR I=3,1,I.G.M+1
            DI(I)=(ST(I,J-1)+ST(I,J+1))*DXY-DX2*WL(I,J)
            F(2)=0
MM          F(I)=(DI(I)+F(I-1))*EJ(I)
            THROUGH NN,FOR I=1,1,I.G.M-1
            J=I4
            H=M+2-I
NN          SF(H,J)=EI(H)*SF(H+1,J)+F(H)
            WHENEVER J.L.N+1,TRANSFER TO HH
             RMAX =0
            THROUGH AAA,FOR I=3,1,I.G.M+1
            THROUGH AAA,FOR J=3,1,J.G.N+1
            WHENEVER((I-4.)/N8-(I-4)/N8).E.0 .AND. ((J-4.)/N8-(J-4)/N8)
           1.E.0
            R3=.ABS.((SF(I,J)+1.0E-30)/(ST(I,J)+1.0E-30))
            WHENEVER RMAX .L.R3,RMAX=R3
AAA         END OF CONDITIONAL
             WHENEVER RMAX .G.EPSLN3
            THROUGH LL,FOR I=3,1,I.G.M+1
            THROUGH LL,FOR J=3,1,J.G.N+1
LL          ST(I,J)=SF(I,J)
```

```
                TRANSFER TO JJ
                OTHERWISE
                 CONTINUE
                END OF CONDITIONAL
                THROUGH ALPHA,FOR I=1,1,I.G.(M+2)
                THROUGH ALPHA,FOR J=1,1,J.G.(N+2)
ALPHA           ST(I,J)=SF(I,J)
                THROUGH BETA,FOR I=2,1,I.G.(M+2)
                 THROUGH BETA,FOR J=2,1,J.G.N+1
                 SF(M+2,J)=-SF(M+1,J)
                U(I,J)=(SF(I,J+1)-SF(I,J))/DY
BETA            V(I,J)=(SF(I,J)-SF(I+1,J))/DX
                WHENEVER NT.L.N2,PRINT RESULTS NT,DT,TIME,U(2,2)...
               1U(M+2,N+2),V(2,2)...V(M+2,N+2),T(1,1)...T(M+2,N+2) ,NE  ,
               2SF(2,2)...SF(M+2,N+2),WL(2,2)...WL(M+2,N+2)    ,RMAX
                 NTO=(NT+0.)/N3-NT/N3
                 WHENEVER NTO.E.0
                 UR=-U(1,2)/2.
                THROUGH CAL,FOR J=3,1,J.G.(N+2)
CAL              UR= UR+U(1,J)
                PRINT RESULTS NT,DT,TIME,UR,U(2,2)...U(M+2,N+2)
               1V(2,2)...V(M+2,N+2),T(1,1)...T(M+2,N+2),SF(2,2)...SF(M+2,N+2)
               2 ,NE   ,WL(2,2)...WL(M+2,N+2)   ,RMAX
                 OTHERWISE
                  CONTINUE
                END OF CONDITIONAL
                WHENEVER T2.G.2,TRANSFER TO GEEM
                WHENEVER T(1,N+2).G.T2,TRANSFER TO LAMDA
                TRANSFER TO BACK
GEEM             WHENEVER NT.L.N7,TRANSFER TO BACK
                 THROUGH AA,FOR I=3,1,I.G.M+1
                THROUGH AA ,FOR J=3,1,J.G.N+1
                WHENEVE  ((I-3.)/N8-(I-3)/N8).E.0 .AND. ((J-3.)/N8-(J-3)/N8)
               1.E.0
                R1=.ABS.((SF(I,J)-ST(I,J))/ST(I,J))
                R2=.ABS.((T(I,J)-TL(I,J))/TL(I,J))
                 WHENEVER R1.G.EPSLON .OR.R2.G.EPSLN2,TRANSFER TO BACK
AA               END OF CONDITIONAL
LAMDA            I3=M/2
                 UR3=-U(I3,2)/2.
                THROUGH LAM,FOR J=3,1,J.G.(N+2)
LAM              UR3=UR3+U(I3,J)
                PRINT RESULTS NT,DT,TIME,UR3,U(2,2)...U(M+2,N+2),
               1V(2,2)...V(M+2,N+2),T(1,1)...T(M+2,N+2),SF(2,2)...SF(M+2,N+2)
               2 ,NE ,RMAX
                 TRANSFER TO START
EE                CONTINUE
                END OF PROGRAM
$ DATA
```

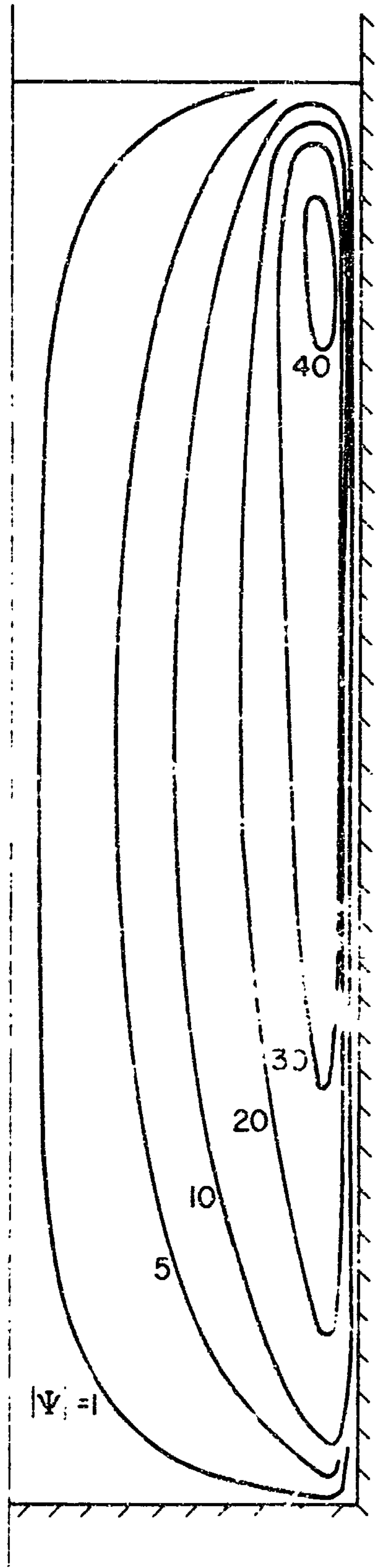

Flow Pattern

wall flux = 10, Btu/hr/ft^2

surface temp. = T_o

$\tau = 6.785 \times 10^{-4}$

≈ 50 sec

21 x 21 grid

Fig. 1

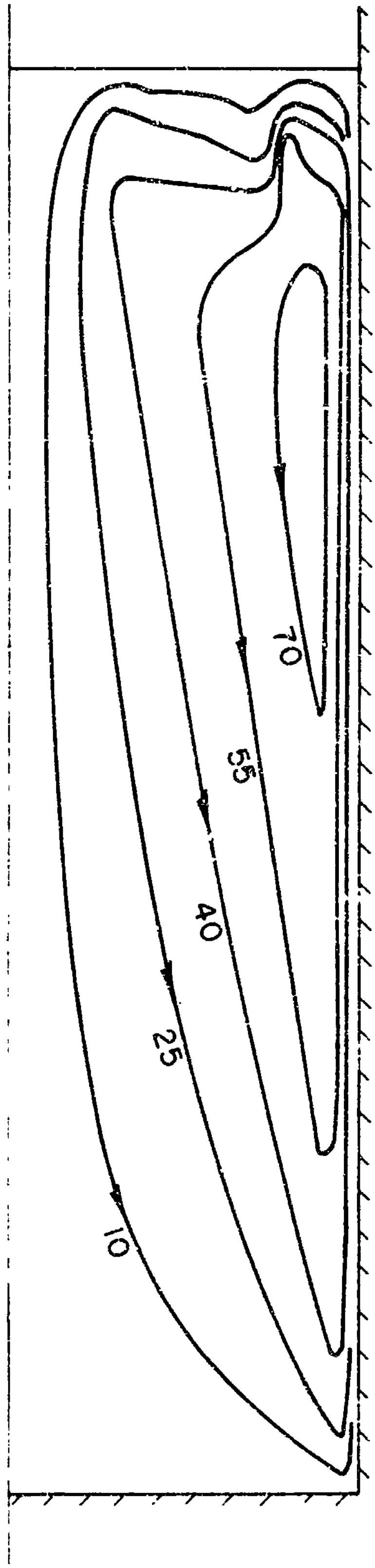

Flow Pattern

wall flux = 10, Btu/hr/ft^2

surface temp. = T_o

$\tau = 1.67 \times 10^{-3}$

≈ 2 min

21 x 21 grid

Fig. 2

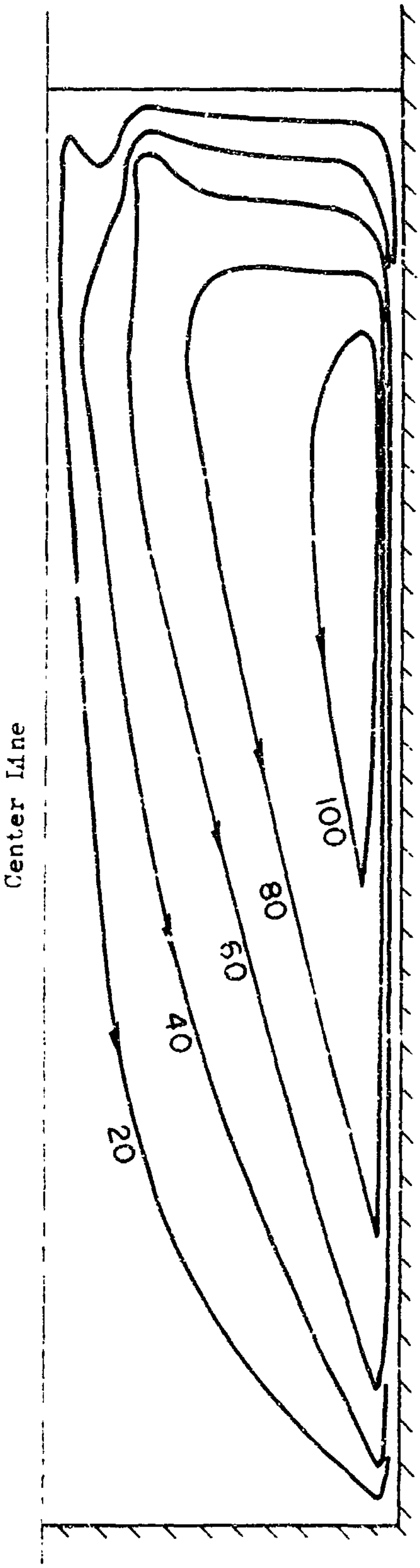

Flow Pattern

wall flux = 10, Btu/hr/ft^2

surface temp. = T_o

τ = .003

≈ 3.6 min

21 x 21 grid

Fig. 3

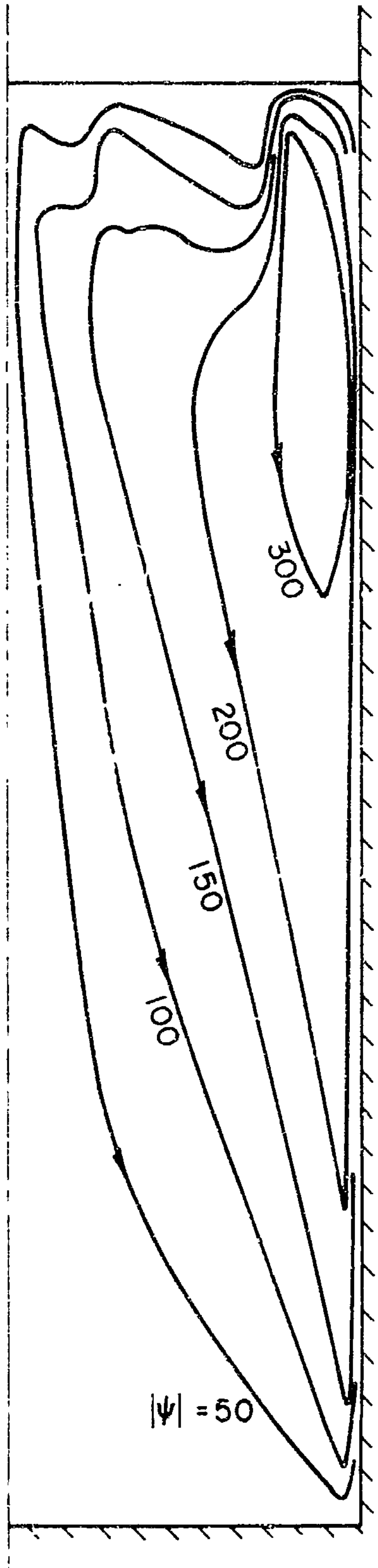

<u>Flow Pattern</u>

wall flux = 1000, Btu/hr/ft^2

surface temp. = T_o

$\tau = 7.07 \times 10^{-4}$

≈ 51 sec

21 x 21 grid

Fig. 4

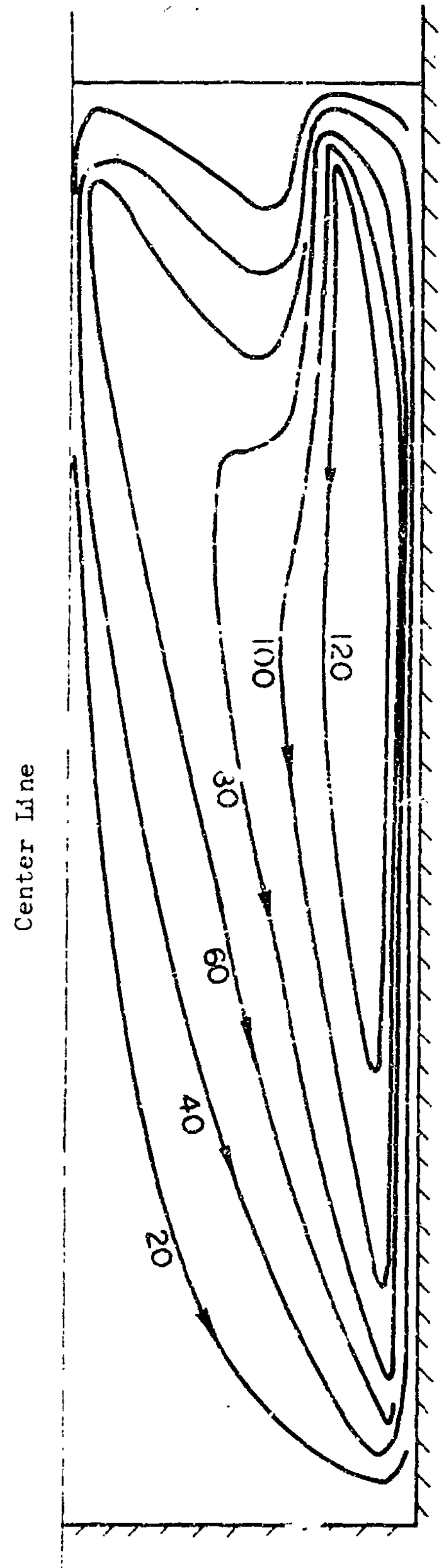

Flow Pattern

wall flux = 10

surface temp. = T_0

τ = .003785

≈ 4.540 min

16 x 16 grid

Fig. 5

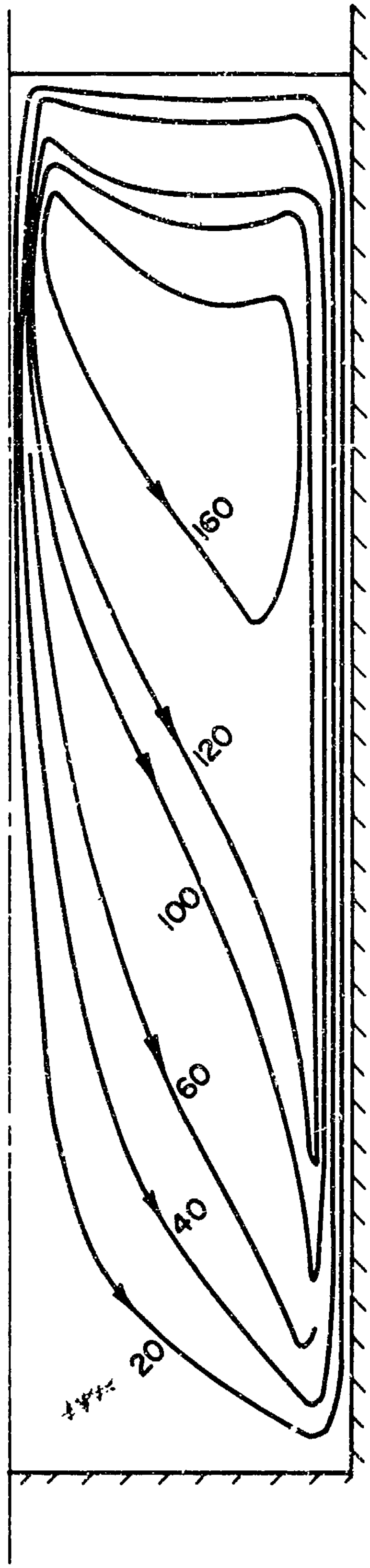

Flow Pattern

wall flux = 10

surface temp. = T_o

τ = .003788

≈ 4.545 min

11 x 11 grid

Fig. 6

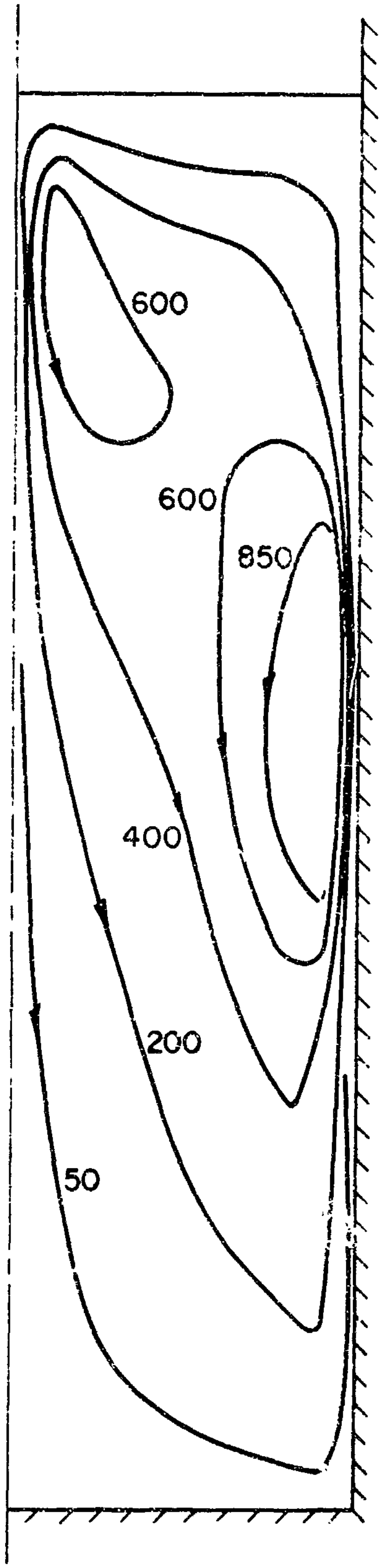

Streamline Pattern

wall flux = 1000 Btu/hr/ft^2

adiabatic upper surface

τ = 0.00114

≈ 3.42 min

11 x 11 grid

Fig. 7

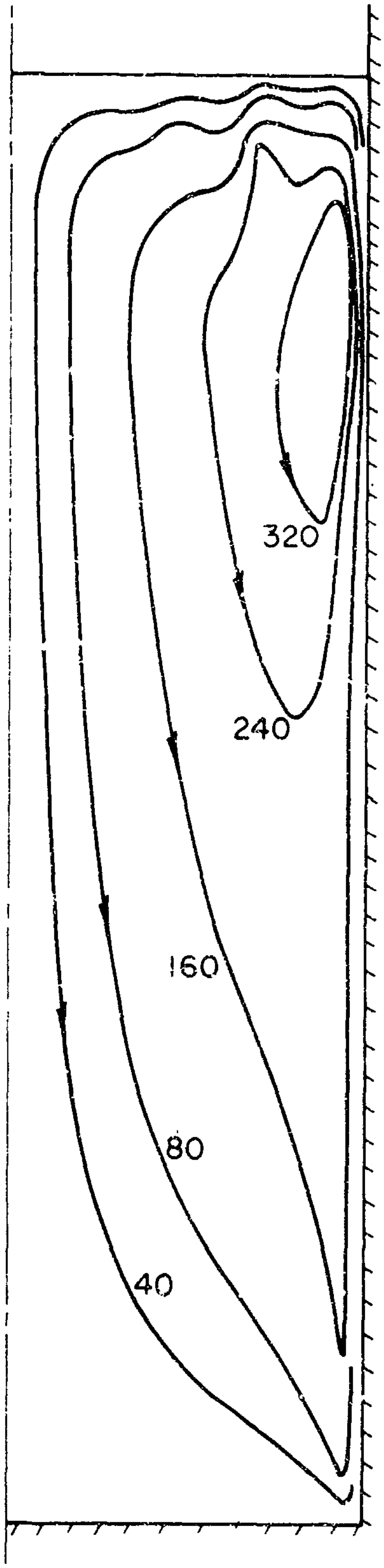

__Streamline Pattern__

wall flux = 1000, Btu/hr/ft^2

surface temp. = T sat.

$\tau = 6.6 \times 10^{-4}$

$\approx$ 48 sec

21 x 21 grid

Fig. 8

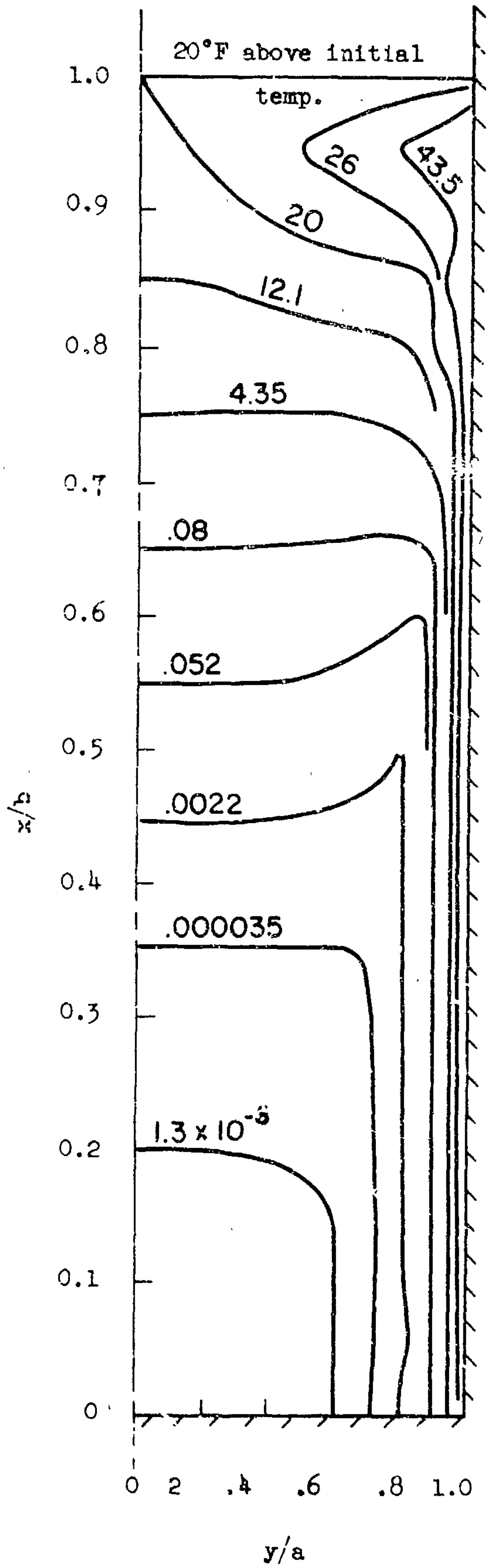

<u>Isothermals</u>

wall flux = 1000, Btu/hr/ft^2

free surface temp. = T_s

τ = 6.6 x 10^{-4}

≈ 48 sec

21 x 21 grid

Fig. 9

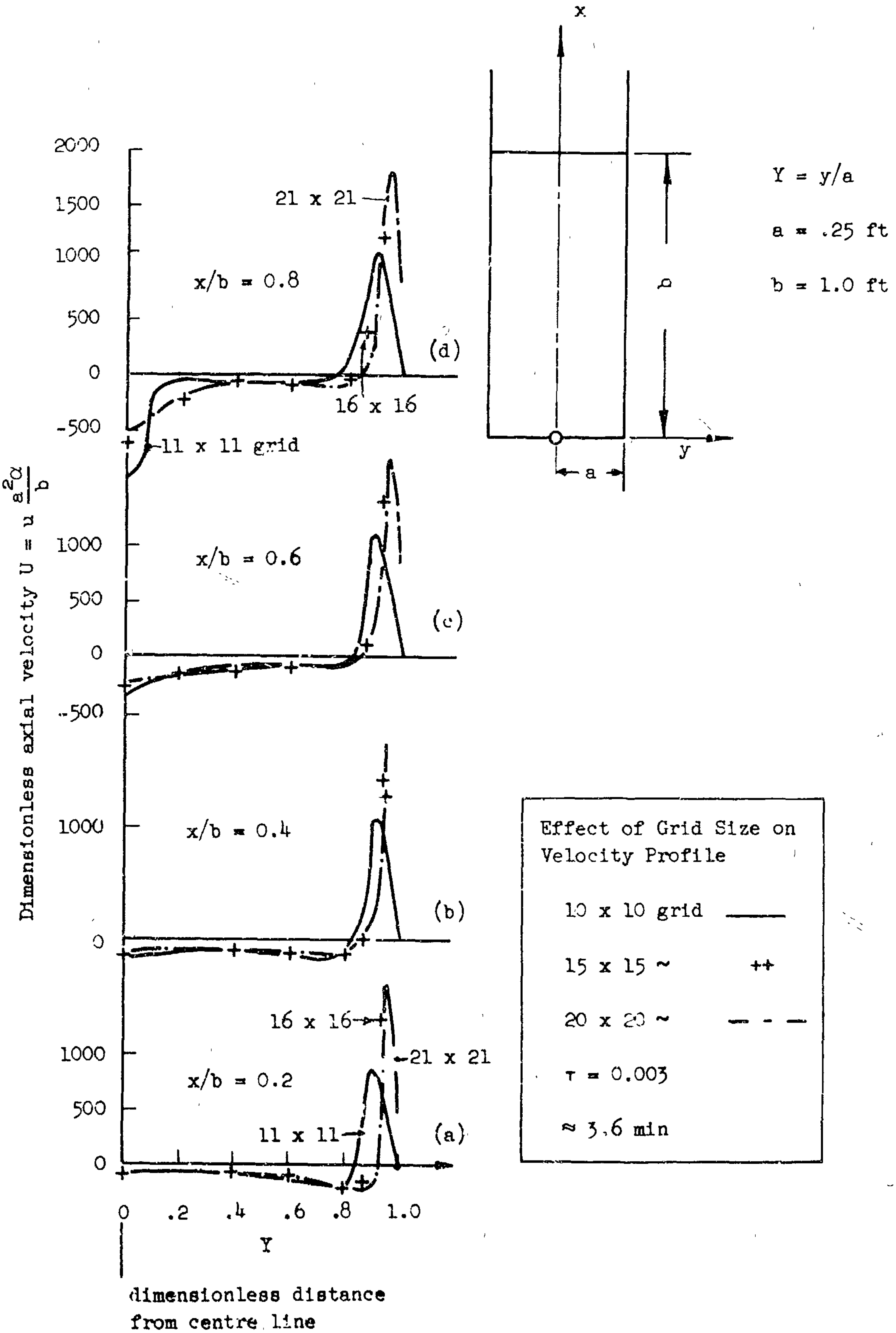

x
Y = y/a
a = .25 ft
b = 1.0 ft
b
y
a
2000
1500
1000
500
0
-500
21 x 21
x/b = 0.8
(d)
16 x 16
11 x 11 grid
x/b = 0.6
(c)
x/b = 0.4
(b)
16 x 16
21 x 21
x/b = 0.2
11 x 11
(a)
0
.2
.4
.6
.8
1.0
Y
dimensionless distance
from centre line
Effect of Grid Size on
Velocity Profile
10 x 10 grid
15 x 15 ~
20 x 20 ~
τ = 0.003
≈ 3.6 min

Fig. 10

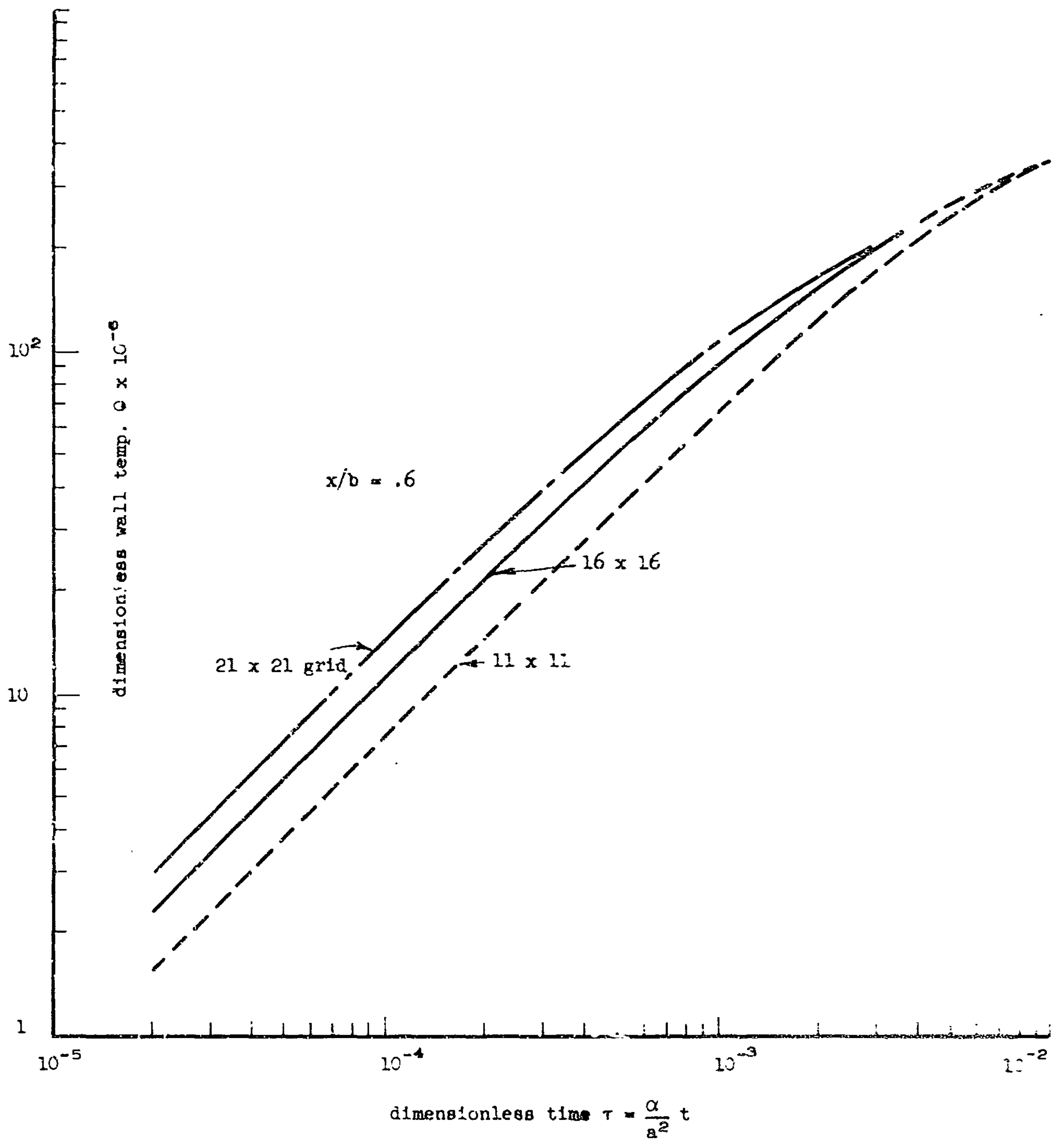
dimensionless wall temp. $\Theta \times 10^{-6}$
10^2
10
1
x/b = .6
16 x 16
21 x 21 grid
11 x 11
10^{-5}
10^{-4}
10^{-3}
10^{-2}
dimensionless time $\tau = \frac{\alpha}{a^2} t$

Fig. 11

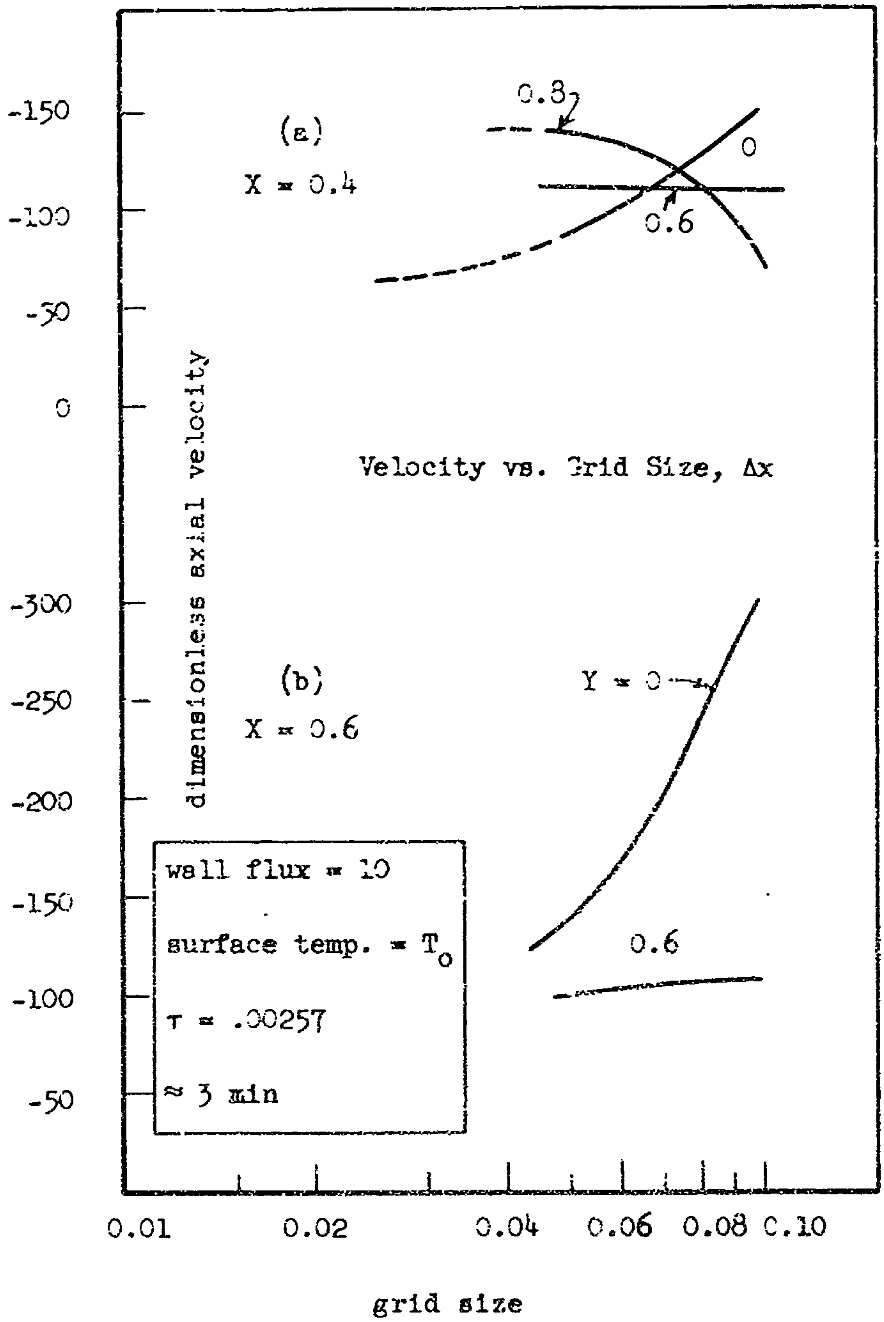

-150
-100
-50
0
(a)
X = 0.4
0.8
0
0.6
Velocity vs. Grid Size, Δx
-300
-250
-200
-150
-100
-50
(b)
X = 0.6
Y = 0
0.6
dimensionless axial velocity
wall flux = 10
surface temp. = T0
τ = .00257
≈ 3 min
0.01
0.02
0.04
0.06
0.08
0.10
grid size

Fig. 12

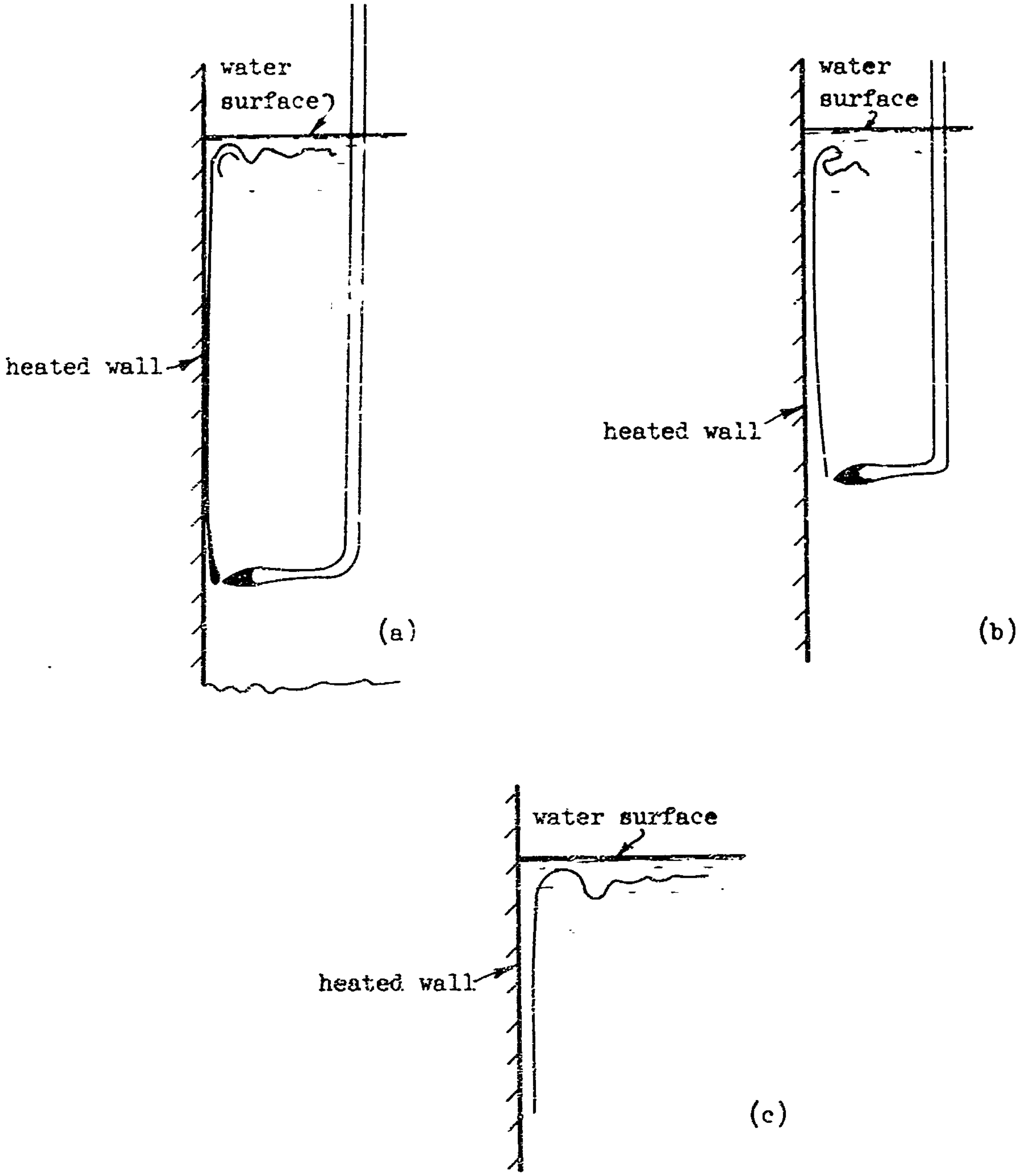
water
surface
heated wall
(a)
water
surface
heated wall
(b)
water surface
heated wall
(c)

Fig. 13

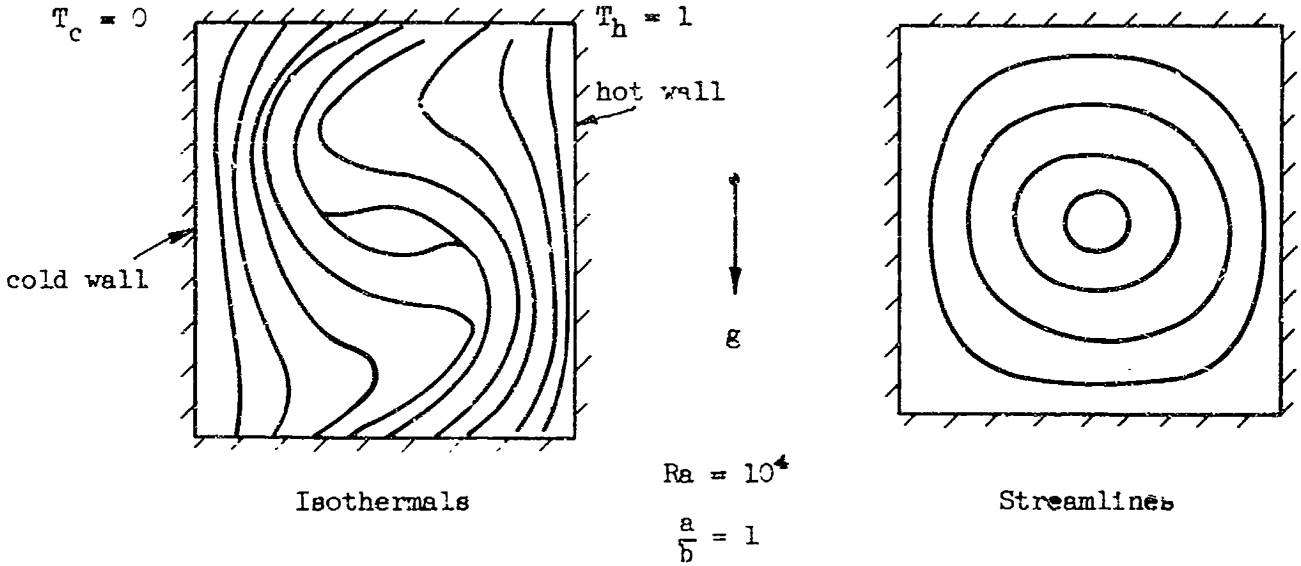
$T_c = 0$
$T_h = 1$
hot wall
cold wall
g
Isothermals
$Ra = 10^4$
$\frac{a}{b} = 1$
Streamlines

Fig. 14